OPERATIONAL EXPERIENCE AND UPGRADING PROGRAM OF THE EXPERIMENTAL FAST REACTOR JOYO

T. AOYAMA, T. ODO, S. SUZUKI, S. YOGO
Japan Nuclear Cycle Development Institute (JNC), Ibaraki, Japan

Abstract

Twenty years of successful operations at the experimental fast reactor JOYO provide a wealth of experience covering core management, chemical analysis of sodium and cover gas for impurity control, natural convection tests, upgrade of fuel failure detection system, corrosion product measurement, development of operation and maintenance support system, and replacement of major components in the cooling systems. Some of the data obtained is stored in a database to preserve the related knowledge. This experience and accumulated data will be useful for the design of future fast reactors.

1. INTRODUCTION

The experimental fast reactor JOYO at the Japan Nuclear Cycle Development Institute's Oarai Engineering Center attained initial criticality in April 1977 and was the first liquid metal cooled fast reactor in Japan. From 1983 to 2000, JOYO operated with the MK-II core as an irradiation test bed to develop the fuels and materials for future Japanese fast reactors. Thirty-five duty cycle operations and thirteen special tests with the MK-II core were completed by June 2000 without any fuel pin failures or serious plant trouble. The reactor is currently being upgraded to the MK-III core. This paper provides a review of the operational experiences obtained through the JOYO's operation.

2. SPECIFICATIONS, PLANT DESCRIPTION AND OPERATION HISTORY OF JOYO

JOYO is a sodium cooled fast reactor with mixed oxide (MOX) fuel. The main reactor parameters of the MK-II irradiation bed core are shown in Table 1, which compares the MK-II with the future MK-III core.

TABLE 1. MAIN CORE PARAMETERS OF JOYO

Items			MK-II	MK-III
Reactor Thermal Output		(MWt)	100	140
Max. No. of Test Irradiation S/A			9	21
Core Diameter		(cm)	73	80
Core Height		(cm)	55	50
^{235}U Enrichment		(wt%)	12(J1)/18(J2)	18
Pu Content		(wt%)	≦30	≦30
Pu fissile Content (Inner/Outer Core)		(wt%)	~20	~16/21
Neutron Flux	Total	(n/cm^2/s)	4.9×10^{15}(J2)	5.7×10^{15}
	Fast(>0.1MeV)	(n/cm^2/s)	3.2×10^{15}(J2)	4.0×10^{15}
Primary Coolant	Temp. (Inlet/Outlet)	(℃)	370/500	350/500
Operation Period		(days/cycle)	45(J1)/70(J2)	60
Reflector/Shielding			SUS/SUS	SUS/B_4C
Max. Excess Reactivity (at 100 ℃)		%Δk/kk'	5.5	4.5
Control Rod Worth		%Δk/kk'	≧9	≧7.6

The MK-II driver fuel plutonium content is about 30wt%. Initially the ^{235}U enrichment was about 12wt%, however this was increased to 18wt% in 1987 to provide enough excess reactivity so that the core burnup was increased. Consequently, the operational period was extended from 45 to 70 days and the plant availability increased. Since 1998, some MK-III driver fuel subassemblies, which have the same specification as the MK-II except a shorter fuel stack length, were loaded in the outer region of the core. Figure 1 shows an example of the MK-II core configuration.

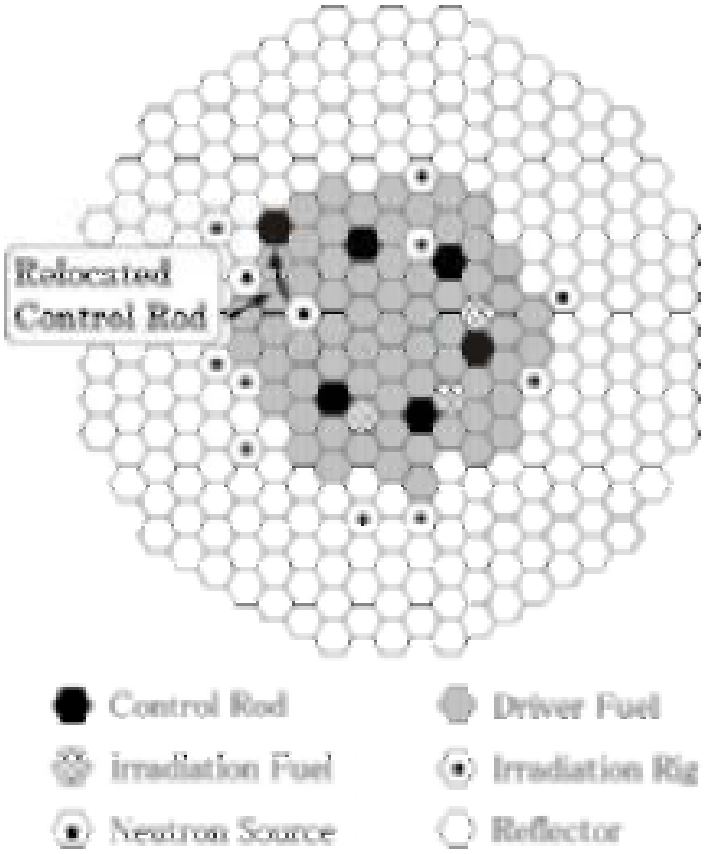

FIG. 1. JOYO MK-II core configuration.

Six-control rod subassemblies made of 90% enriched B_4C were used in JOYO MK-II and were located symmetrically in the third row. In 1994, one control rod was moved to the fifth row to provide a position for irradiation test assemblies with on-line instrumentation. Since then, the control rod subassemblies have been loaded asymmetrically. The JOYO cooling system has two primary sodium loops, two secondary loops and an auxiliary cooling system. The cooling system uses approximately 200 tons of sodium. In the MK-II core, sodium enters the core at 370°C at a flow rate of 1 100 tons/h/loop and exits the reactor vessel at 500°C. The maximum outlet temperature of a fuel subassembly is about 570°C. An intermediate heat exchanger (IHX) separates radioactive sodium in the primary system from non-radioactive

sodium in the secondary system. The secondary sodium loops transport the reactor heat from the IHX to the air-cooled dump heat exchanger (DHX). A flow diagram of the cooling system of MK-II core is shown in Fig. 2.

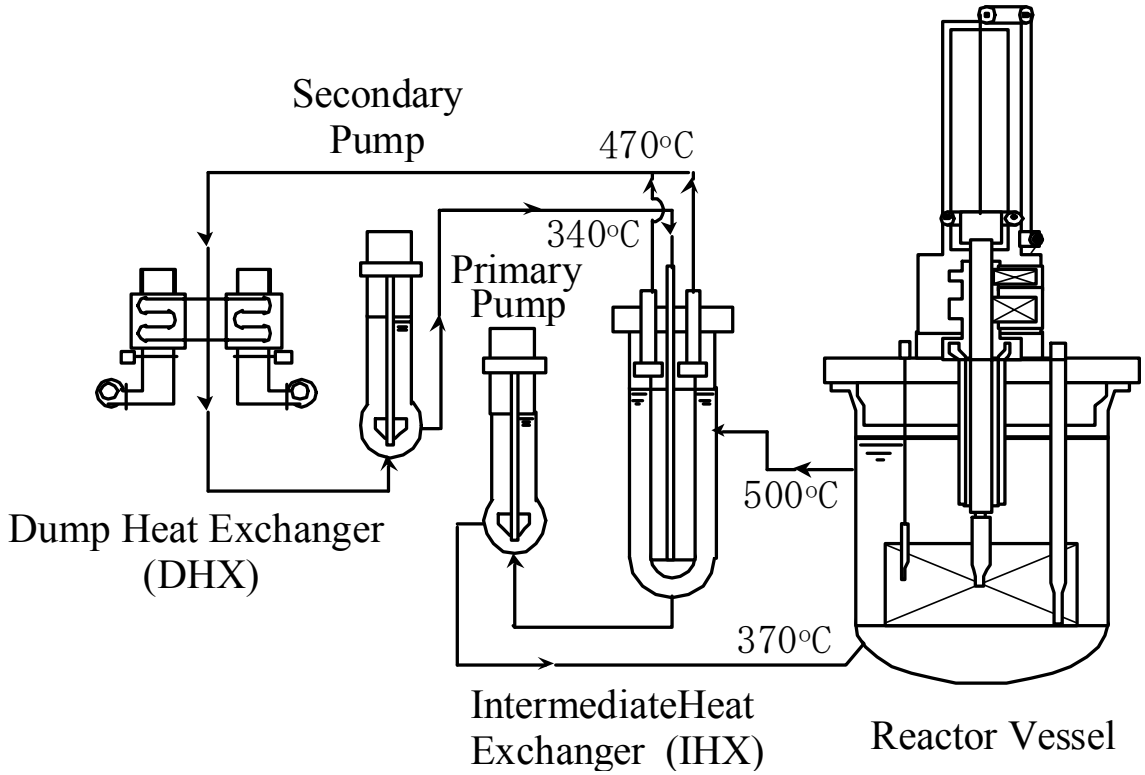

FIG. 2. JOYO cooling system diagram.

The operating data and history of the JOYO MK-II core are shown in Table 2 and Fig. 3. The reactor operated for 48 000 hours and the integrated power generated was 4 400GWh. During the MK-II operation, 382 driver fuel subassemblies and approximately 47 000 fuel pins were irradiated. A peak burnup value of 86.0 GWd/t was attained for the MK-II driver fuel without any fuel pin failures.

TABLE 2. JOYO MK-II OPERATING DATA

Operation Time(Accumulated)	48,000 hrs
Heat Generation(Accumulated)	4,400 GWh
Max. Fuel Burn-up	
Driver Fuel	86 GWd/t
Irrad. Fuel	142 GWd/t
No. of Irradiated Fuel Subassemblies	382

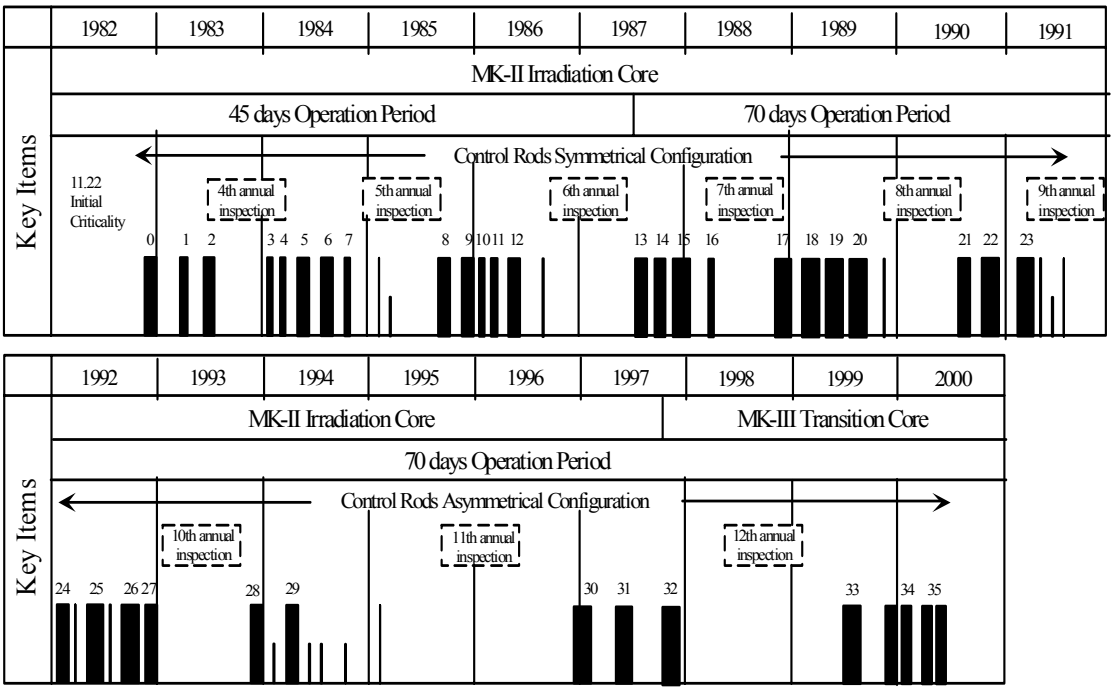

FIG. 3. JOYO MK-II core operation history.

3. CORE MANAGEMENT EXPERIENCE

A core management code system has been developed to predict the core parameters for operation and refueling plans within the design limitations. The nuclear calculation is based on diffusion theory and corrected with a bias method. Results from core physics tests and Post Irradiation Examinations (PIE) have been used to confirm the accuracy of these predictions. These verifications are also important to conduct various irradiation tests accurately. This section describes the method and verification for core and fuel management used with the JOYO MK-II core.

3.1. Method

The MAGI calculation code system [1, 2] was developed to predict the reactor parameters required for core and fuel management of the JOYO MK-II core.. MAGI is a neutronic and thermo-hydraulic coupling code system that calculates the excess reactivity, power distribution, fuel burnup, coolant flow rate and temperature condition of each subassembly. MAGI uses diffusion theory with seven neutron energy groups for the nuclear calculations. The neutron cross section was collapsed from the 70 group JFS-3-J2 cross section set [3] processed from the JENDL-2 library. It was updated to the JFS-3-J3.2 cross section set based on the JENDL-3.2 library [4] in 2001. The gamma-ray cross section that includes delayed fission gamma-ray was processed from the JENDL-2 library to improve the calculations of gamma heating in stainless steel. The core configuration was modeled in three-dimensional Hex-Z geometry for each operational cycle. The actual reactor power history was used in the burnup calculation. Figure 4 shows the MAGI system outline.

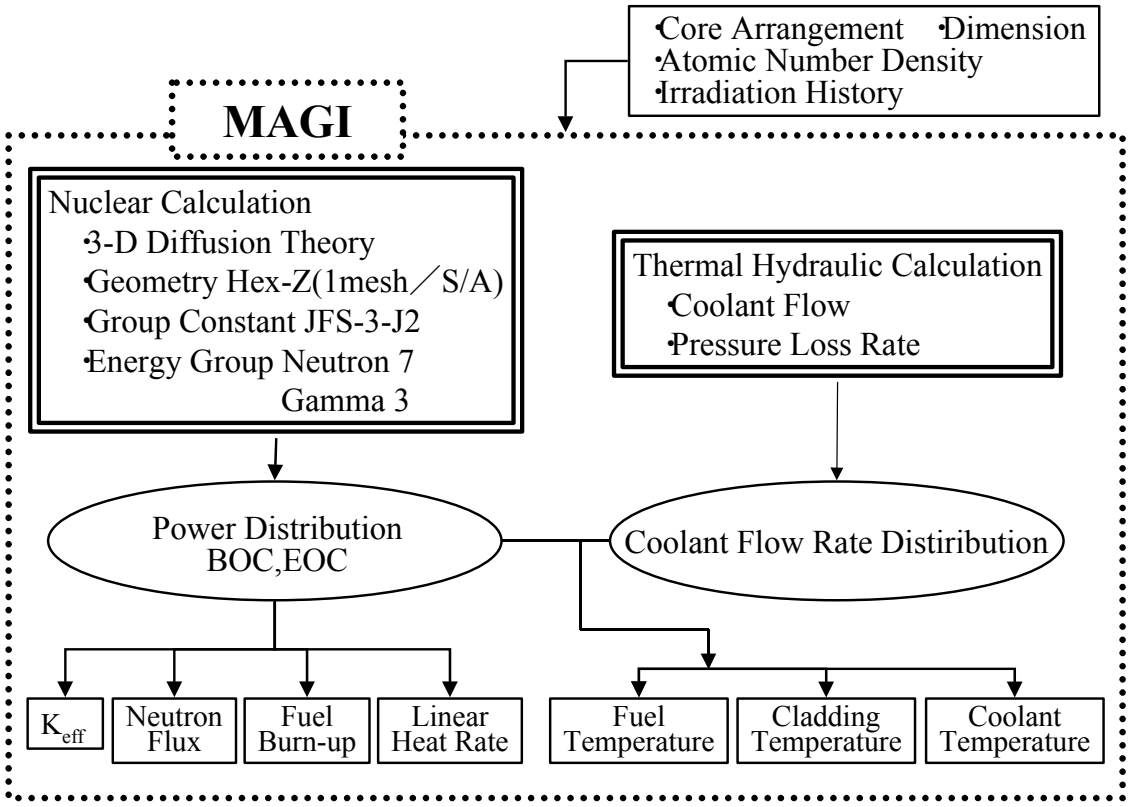

FIG. 4. JOYO MK-II core management code system.

MAGI supported the refueling plan for each operational cycle. The number of fresh driver fuel subassemblies and their position were determined within design limitations of neutronic and thermal parameters with consideration for the following items:

(1) Burnup of fuel subassembly;
(2) Operation period of the cycle;
(3) Neutron fluence and temperature condition of the irradiation test subassemblies.

The number of discharged spent fuel subassemblies ranges from 10 to 12, about one sixth of total driver fuel subassemblies. The frequent refueling affects the core characteristics and irradiation conditions significantly so the MAGI calculation needs to be verified in each operation cycle.

3.2. Verification of core management

3.2.1. Core physics tests in each operational cycle

3.2.1.1. Criticality and burnup reactivity

The excess reactivity in a zero power critical condition was measured at the reactor start-up of each operational cycle. Measured data were compared with the MAGI calculated values that included the bias factor (C-E) correction obtained for the previous cycle. The comparison of calculated and measured values is shown in Table 3.

TABLE 3. C/E VALUES OF CORE CHARACTERISTICS

Core Characteristic	C/E
Excess Reactivity (%Δk/kk')	0.99±0.03
Control Rod Worth	(±0.1%Δk/kk')
Symmetrical (%Δk/kk'/total)	0.99±0.02
Asymmetrical (%Δk/kk'/total)	0.98±0.01
Burn-up Reactivity Coefficient (%Δk/kk'/MWd/t)	0.96±0.05

By using this bias method, it was found that the excess reactivity after refueling can be well predicted within an error of 0.1%Δk/kk'. The burnup reactivity was determined by measuring the reactivity change during rated power operation. Measured values were compared with the MAGI burnup calculation and both agreed within 5% as shown in Table 3.

It is considered that the decrease of atomic number densities of major fissile nuclides as ^{235}U and ^{239}Pu are the dominant factor of burnup reactivity because of JOYO's small core size, which results in hard neutron spectrum and small internal conversion ratio (~0.3). Therefore, the burnup reactivity can be predicted accurately even at a high burnup.

3.2.1.2. Control rod worth

Every control rod's worth was calibrated with either the positive period method or the inverse kinetics method during the low power test of each operational cycle. The calculation was conducted with the CITATION code based on three dimensional diffusion theory using the same cross section, geometry and atomic number densities as MAGI. After correcting with the previous cycle's C/E, the calculated values were compared with the measurements.

Table 3 shows that both agreed within 2%. When one control rod was moved from the third row to the fifth row in 1992, the worth of the relocated rod was reduced to one third. The calculation accuracy was not changed significantly.

3.2.1.3. Reactivity coefficients

Reactivity coefficients are important for safety reasons and to account for the reactivity change associated with temperature and power changes during reactor operation. The measured values are used to predict the reactivity change for the next operational cycle.

The isothermal temperature coefficients were measured by taking the difference of reactivity at approximately 250 and 370°C during reactor start-up. The measured isothermal temperature coefficients were constant through the MK-II operation because they were determined mainly by radial expansion of the core support plate, which is independent of burnup. However, when the core region was gradually extended from the 32^{nd} cycle, the isothermal temperature coefficients were decreased as predicted with the mechanism. Table 4 shows these values.

TABLE 4. MEASURED ISOTHERMAL TEMPERATURE COEFFICIENTS

Cycle	Number of Fuel S/A	Isothermal Temperature Coefficient ($\times 10^{-3}\%\ \Delta k/kk'/^{\circ}C$)
MK-II Average	67	-3.98± 0.12
32	69	-3.67
33	71	-3.65
34	75	-3.47
35	76	-3.49

The power coefficients were measured at the reactor start-up and shutdown in each operational cycle. Figure 5 shows that the measured power coefficients decreased with increasing core burnup.

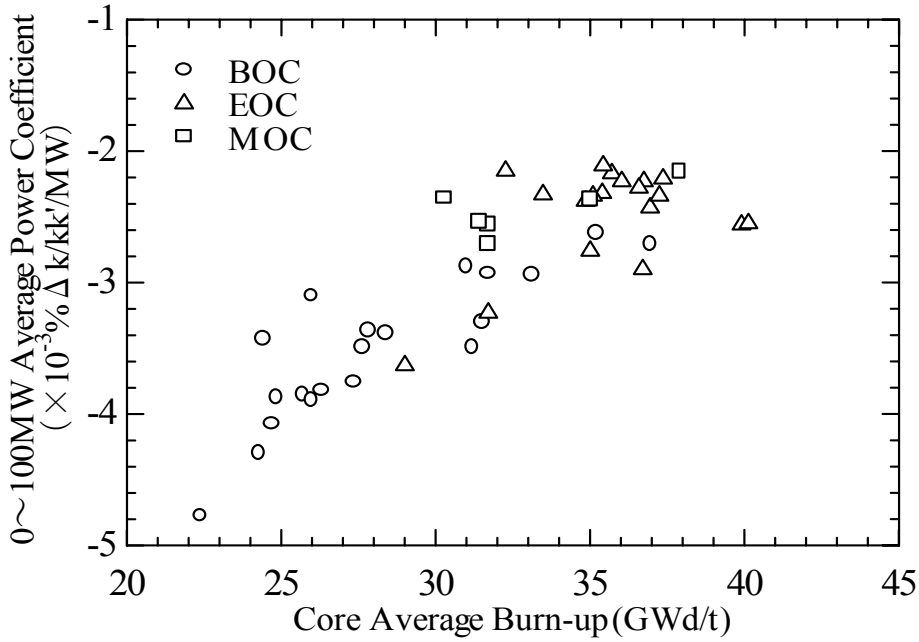

FIG. 5. Burnup dependence of power coefficient.

It was considered that the fuel thermal expansion, which is the major component of the power coefficient of JOYO, decreases at high burnup due to fuel restructuring during irradiation. It was also observed that the power coefficients varied depending on the reactor power as shown in Fig. 6. This phenomenon appeared to be due to a combination of the core bowing effect, fuel thermal expansion and Doppler effects. These causes need further investigation.

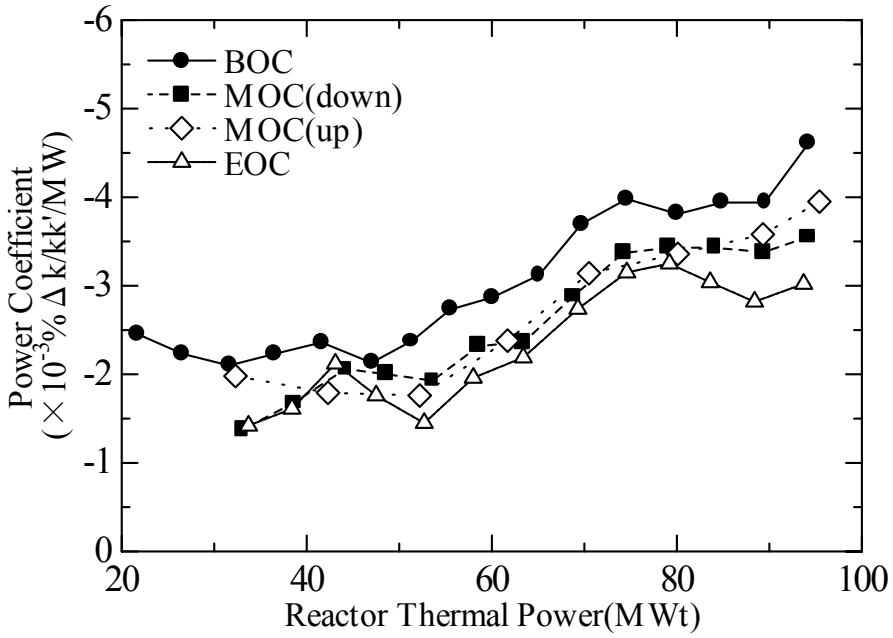

FIG. 6. Power dependence of power coefficient.

3.2.2. Post Irradiation Examination (PIE)

3.2.2.1. On-site burnup distribution measurement

The calculation accuracy of MAGI's axial power distribution was confirmed by comparing the relative distribution of measured (^{144}Pr) and calculated fuel burnup. The burnup measurement was taken in the JOYO spent fuel storage pond [5]. The spent fuel subassembly was contained in a stainless steel can, and it was set on a fuel-scanning device. Axial and circumferential gamma-ray distributions were measured using a high purity germanium (Ge) detector by moving the fuel scanning system vertically and by rotating the subassembly around the fixed detector.

As illustrated in Fig. 7, the MK-II spent fuel subassembly with a burnup of 62.5 GWd/t and cooling time of 5.2 years was measured. It was shown that the measured and MAGI calculated values were close except at the upper region of the fuel column. This difference was apparently due to the calculation error of neutron absorption by control rod.

3.2.2.2. Burnup ratio measurement by ^{148}Nd method

Chemical analysis of ^{148}Nd was conducted at the hot cell facility. As ^{148}Nd is one of the stable fission products and its fission yield is highly reliable, ^{148}Nd production obtained by destructive examination has been commonly used as a burnup index [6]. The calculated and measured burnup ratios for the MK-II spent fuel from 0.3 to 8.7 atom% is shown in Fig. 8. Measured results agreed with the MAGI burnup calculation within 5% in each row.

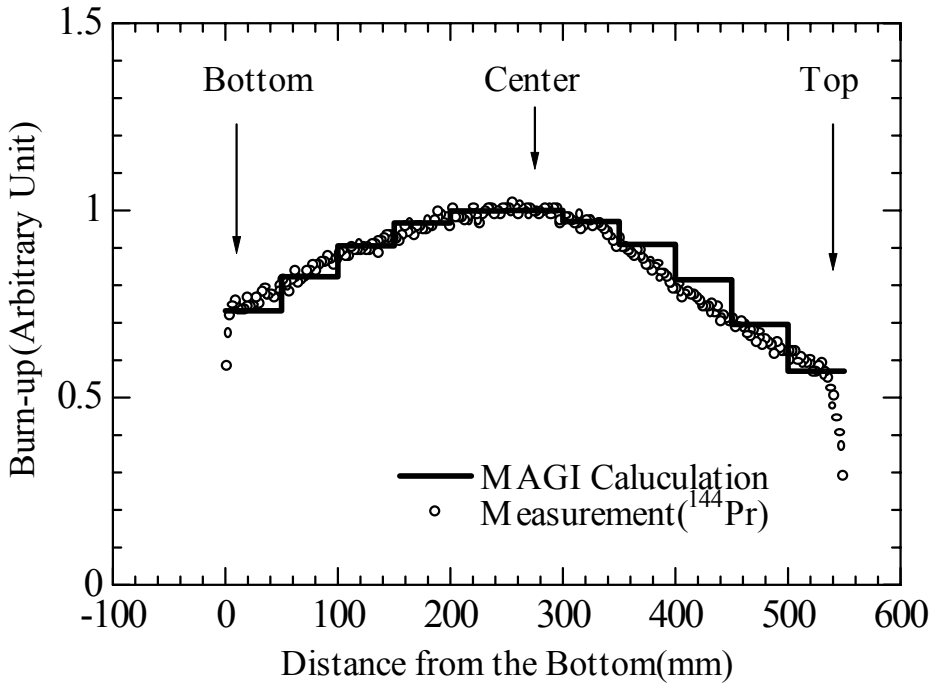

FIG. 7. Axial burnup distribution of JOYO MK-II driver fuel.

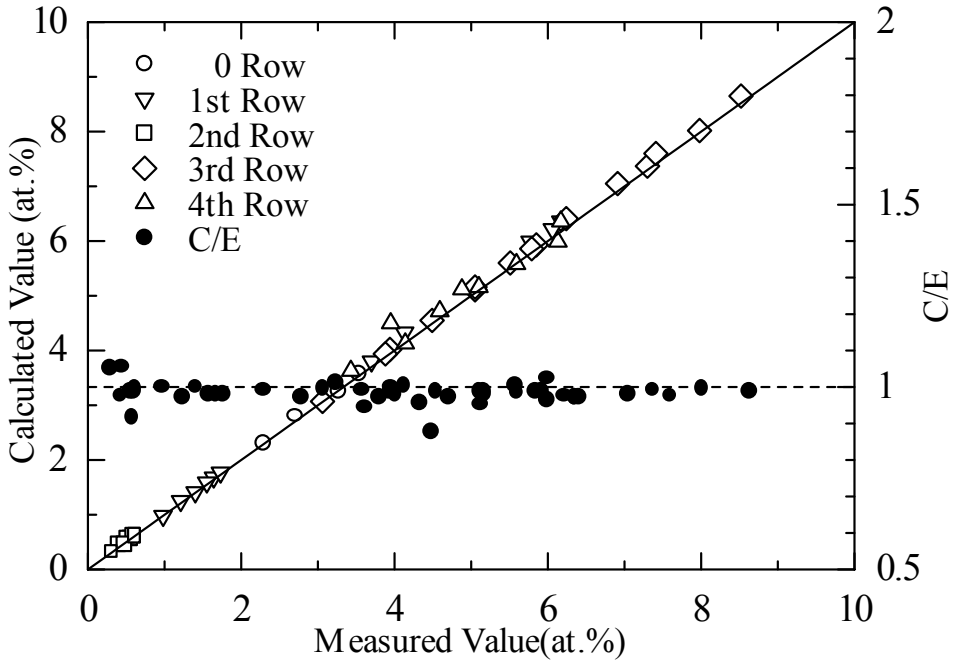

FIG. 8. Burnup ratio of JOYO MK-II driver fuel.

3.2.2.3. Decay heat measurement

The accuracy of decay heat calculations depends on the individual heat generation rate from fission product decay nuclides and actinides, and the burnup calculation for its production and transmutation. To obtain experimental data and to improve the accuracy of related calculations, the decay heat of MK-II spent fuel subassemblies was measured at the JOYO spent fuel storage pond [7]. The fuel burnup was approximately 66 GWd/t and the cooling time was between 40 and 385 days. The measured decay heat is shown in Fig. 9.

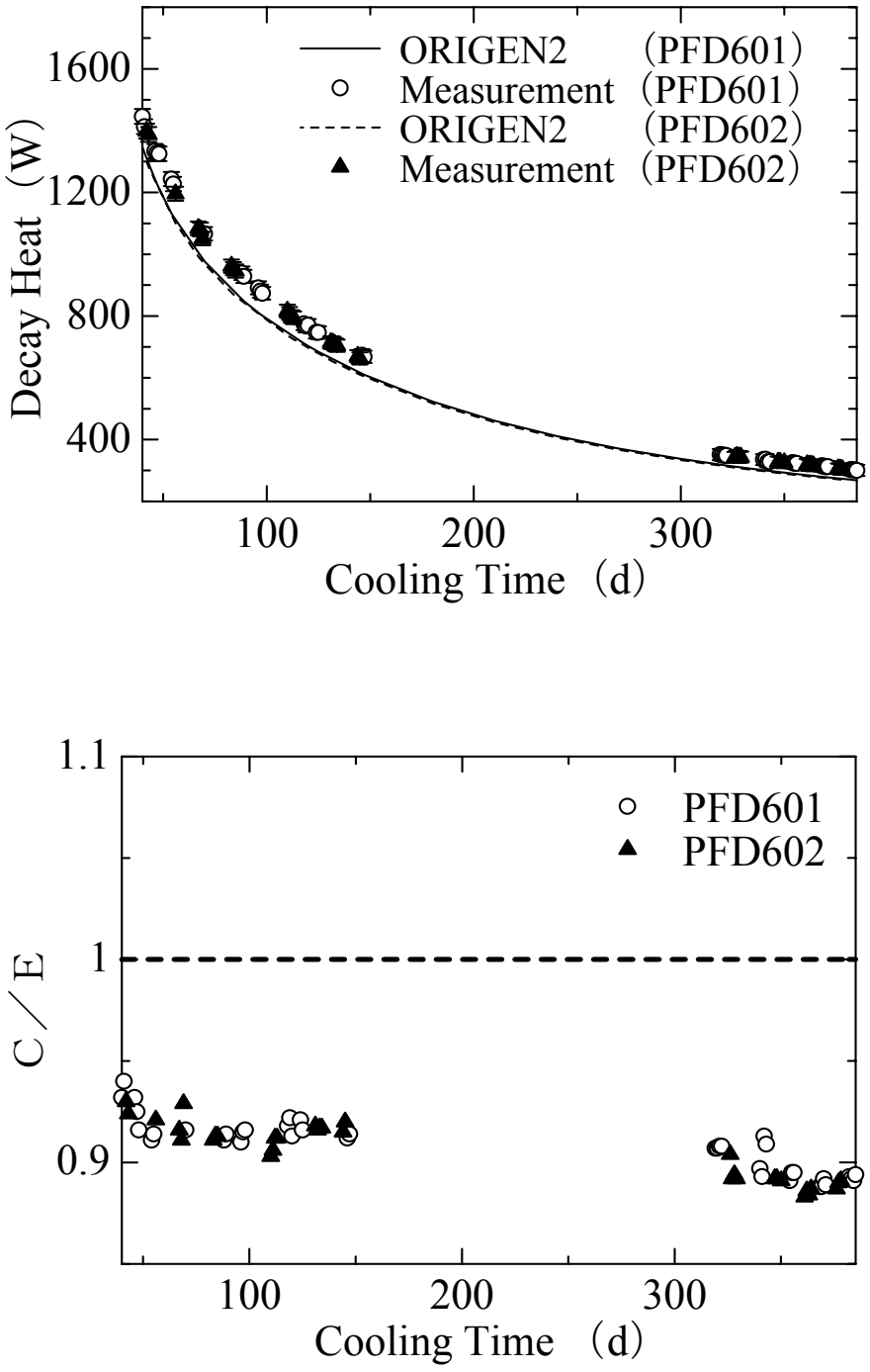

FIG. 9. Measured and calculated decay heat of JOYO MK-□ spent fuel.

The decay heat was then calculated with the ORIGEN2 code using the JENDL-3.2 cross section library and the JNDC-V2 [8] decay data and fission yield data library. The fuel power used as an input to ORIGEN2 was calculated by MAGI. The ratios of calculated to experimental values were between 0.94 and 0.89, and decreased with a longer cooling time as shown in Fig. 9. This systematic discrepancy needs to be further investigated, but the change with cooling time appears to be due to the actinides' decay heat uncertainty. Table 5 shows calculated and adjusted neutron flux and fluence.

TABLE 5. CALCULATED AND ADJUSTED NEUTRON FLUX AND FLUENCE

Item	Adjusted Value (NEUPAC)	MAGI	MAGI/ NEUPAC
(Core Region)	(1σ Error)		
ϕ_{total} (n/cm^2/s)	3.97×10^{15} (4.8%)	4.18×10^{15}	1.05
$\phi_{>0.1MeV}$ (n/cm^2/s)	2.61×10^{15} (8.0%)	2.83×10^{15}	1.08
DPA (dpa/s)	1.27×10^{-6} (5.0%)	---	---

3.2.3. Reactor dosimetry

The neutron flux calculation error rate was evaluated to be less than 5% in the fuel region according to the comparison between MAGI and reactor dosimetry test results (see Table 5). Figure 10 shows an example of adjusted neutron spectrum based on the foil activation method at the core center position of the MK-II.

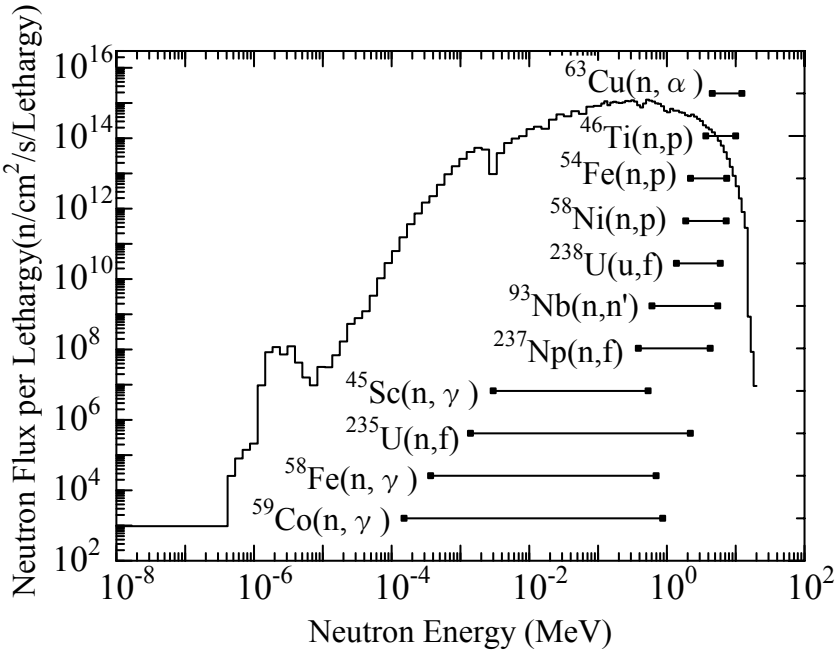

FIG. 10. Adjusted neutron spectrum at JOYO MK-II core center.

The dosimetry test results were used to correct MAGI calculations to assure the neutron fluence used in the post irradiation test analysis (see Table 5). A Helium Accumulation Fluence Monitor (HAFM) has been developed to improve the accuracy of long-term irradiation tests.

3.3. MK-II core characteristics database

During the MK-II operation, extensive data were accumulated from start-up and core characteristics tests. These core management and core characteristics data were compiled into a database [2]. The core management data includes core specifications and configurations, atomic number densities before and after irradiation, neutron and gamma flux, neutron fluence, fuel burnup, and temperature and power distributions. The core characteristics data include excess reactivities, control rod worths, and reactivity coefficients, e.g., temperature, power and burnup. These core characteristics data were recorded on CD-ROM for user convenience.

4. CHEMICAL ANALYSIS OF SODIUM AND COVER GAS

It is essential for steady and safe operation of a sodium cooled fast reactor to limit the coolant and cover gas impurities to prevent corrosion of reactor component materials and to reduce radiation dose by corrosion products (CPs). Therefore, impurity concentrations of both coolant sodium and cover gas argon were measured during the duty cycle operation and annual inspection period. The sodium impurity data include oxygen, hydrogen, nitrogen, chloride, tritium, metal elements and radioactive ^{110m}Ag, ^{22}Na, ^{137}Cs. The cover gas impurity data include O_2, N_2, CO, CO_2, H_2, CH_4, He, ^3H and radioactive xenon and krypton isotopes.

These data were measured by chemical analysis, gas chromatography, beta-ray scintillation and gamma-ray spectrometry. The sodium impurity concentrations were also determined by the sodium temperature in the plugging indicator. As an example, the trend of oxygen and hydrogen in the primary sodium are shown in Fig. 11.

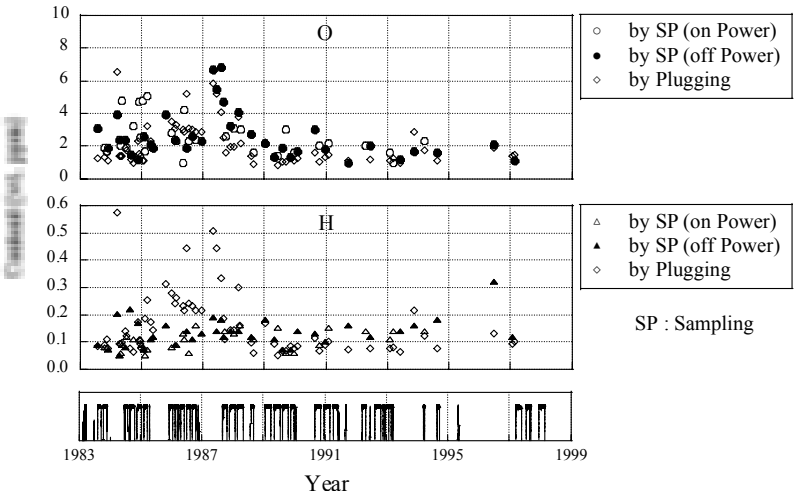

FIG. 11. Hydrogen and oxygen content in JOYO primary coolant sodium.

5. DECAY HEAT REMOVAL TEST OF NATURAL CONVECTION

The inherent safety of a fast reactor can be demonstrated by proving the natural convection capability and establishing analytical techniques based on experiments. A series of natural convection tests was performed from 1981 to 1986 in JOYO. The natural convection test from 100 MWt, which is the most critical situation for the reactor, was carried out at the end of 12th cycle of the MK-II core in 1986 [9]. The test was initiated by tripping primary and secondary sodium pumps manually without pony motor operation, and the reactor was shut down simultaneously by tripping the pumps; moreover, the blowers of the DHXs were stopped immediately with the reactor scram signal. The central driver fuel subassemblies undergo the most severe temperature transition during the tests. Figure 12 shows the outlet temperature of one of these assemblies, together with primary coolant flow rate variations. The peak temperature reached 519°C due to coolant flow rate reductions. This peak is significantly below the initial temperature of 548°C. Consequently, it is shown that the temperature increase will not cause any safety-related problems, such as fuel cladding failure.

The post analysis results from a plant wide dynamics code MIMIR-N2 are in excellent agreement with the experimental data as shown in Fig. 12. Various key parameters are clarified to improve the calculation accuracy through the study. In the short-term analysis, the evaluation of thermo-hydraulic behavior in the core is largely affected by the inter-assembly heat transfer effect, the pump flow coast characteristics and coolant flow distribution. For the long-term analysis, it is important to assess precisely the buoyant head effect in the IHX, the heat exchange effects in the lower plenum of the IHX and others. The experimental result is also applied to the assessment of natural convection characteristics in the MONJU reactor.

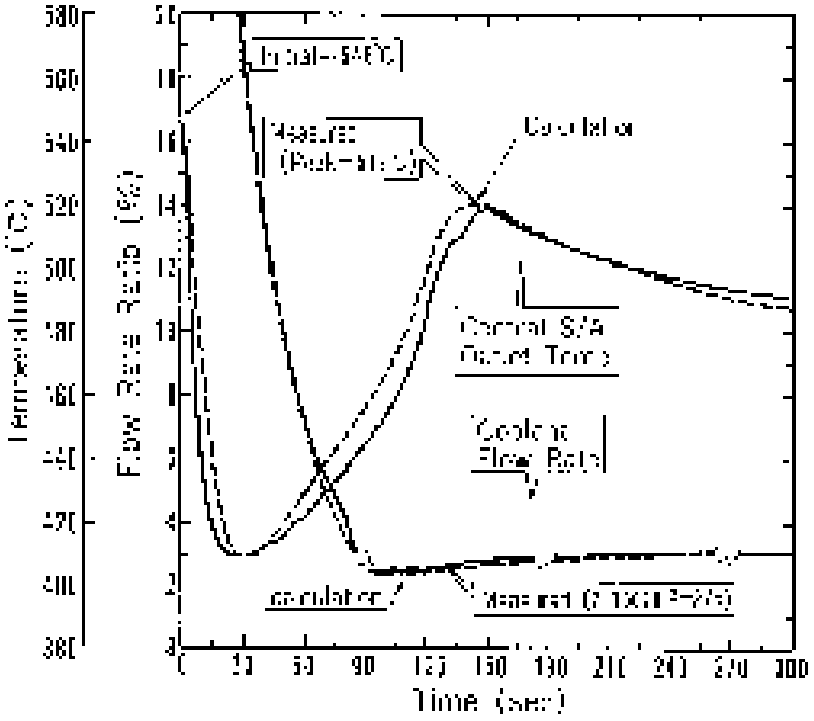

FIG. 12. Test results and analysis of neutral convection test.

6. UPGRADE OF FFD SYSTEM AND INSTALLATION FP TRAPS

The fuel failure detection (FFD) and the failed fuel detection and location (FFDL) are important for LMFBR plants to achieve high availability and operational reliability. Fission product (FP) traps are important for safety reasons: especially for conducting safe Run-beyond-cladding-breach (RBCB) tests.

The JOYO FFD system consists of both delayed neutron (DN) monitoring systems and a cover gas (CG) precipitating system. The schematic diagram of the JOYO FFD system is illustrated in Fig. 13.

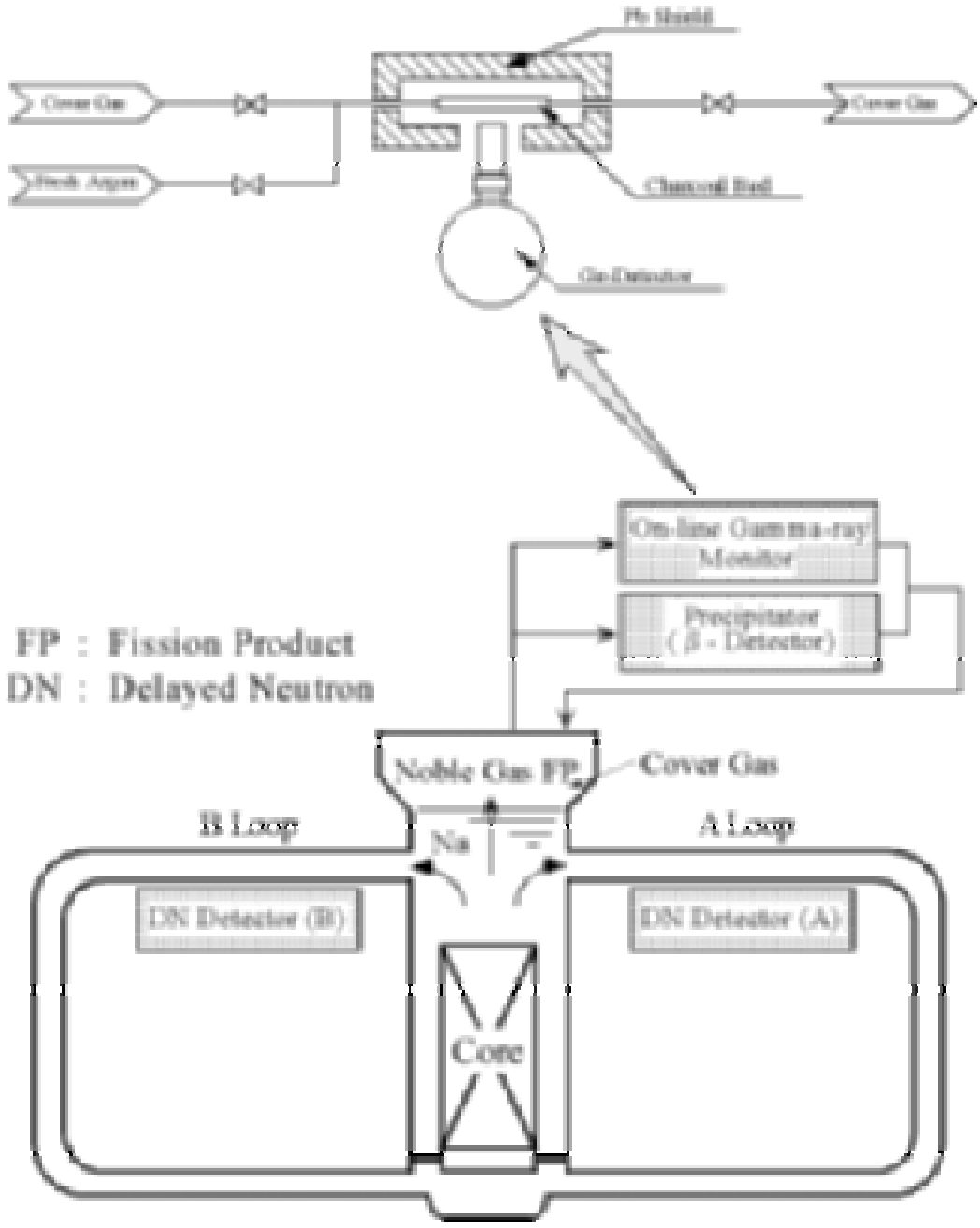

FIG. 13. Schematic diagram of JOYO FFD system and OLGM.

Ttwo DN monitoring systems are located adjacent to the primary cooling loops to detect the delayed neutrons emitted from precursors released into the coolant sodium. The CG precipitating system detects fission product of ^{88}Rb i.e. beta decay of ^{88}Kr released into the cover gas argon.

A Run-to-Cladding-Breach (RTCB) test is planned in JOYO. The RTCB test is expected to improve the FBR fuel performance. The results will increase the fuel burnup and extend the cladding life-time. As part of the preparation work, the FFD system has been upgraded to improve its accuracy and reliability and FP traps have been installed. A series of simulated fuel failure tests has been conducted [10].

6.1. Upgrade of the FFD system

6.1.1. On-line gamma-ray monitor

The On-line Gamma-ray Monitor (OLGM), shown in Fig. 13, has been developed and installed in JOYO.

The OLGM consists of a charcoal bed that is made to selectively adsorb the isotopes of krypton and xenon, and a high purity Ge detector. The special feature of this system is to be able to identify the isotopes in the cover gas by means of gamma-ray spectrum analysis. The OLGM is also used to detect the tag gas that is originally contained inside a pressurized stainless steel capsule. In the irradiation environment, the creep rupture may cause the capsule to fail and release the tag gas into the cover gas. As shown in Fig. 14, the activated tag gas nuclides among the background fission products are clearly detected by OLGM and this method was found to be applicable [11].

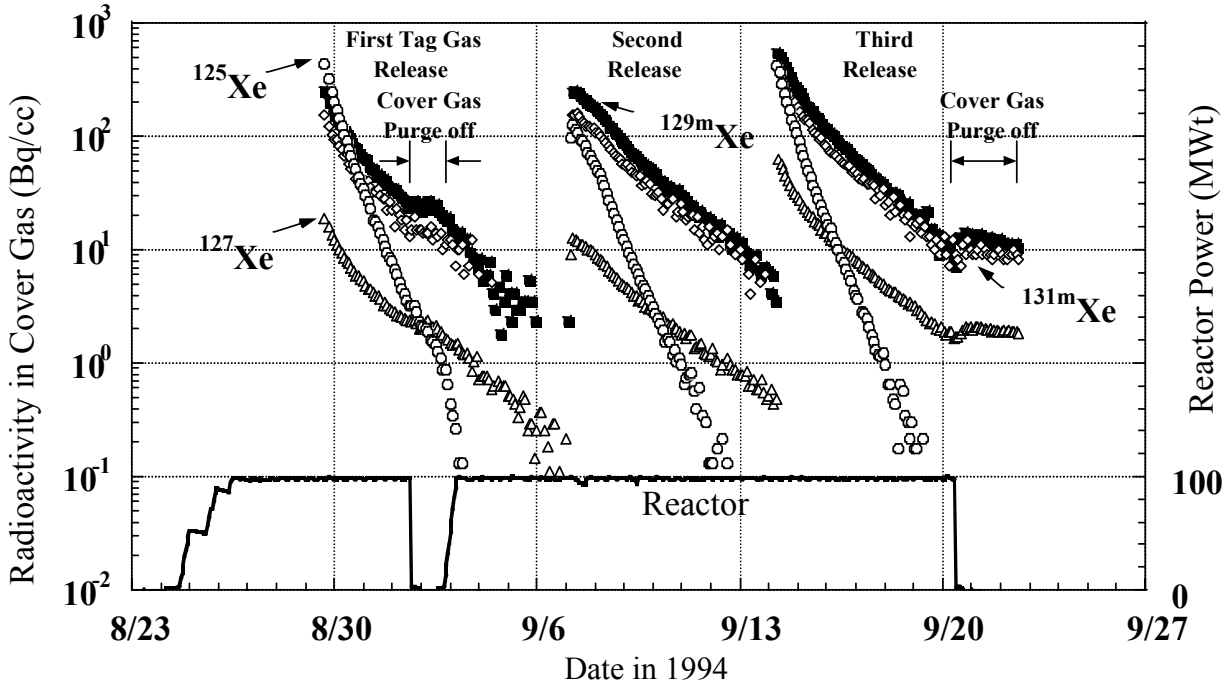

FIG. 14. Measured tag gas activation products in JOYO.

6.1.2. Resonance ionization mass spectrometry

The Resonance Ionization Mass Spectrometry (RIMS) is a method to detect xenon and krypton with ultra high sensitivity using a laser technique [12] developed in collaboration with the University of Tokyo and Nagoya University. The block diagram of a RIMS system with a time of flight (TOF) mass spectrometer is illustrated in Fig. 15.

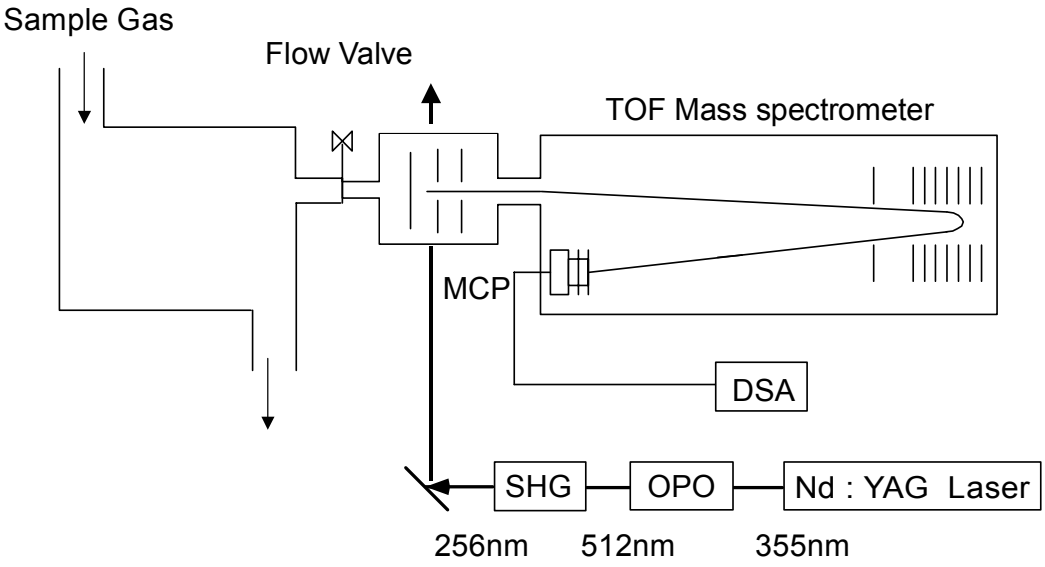

RIMS: Resonance Ionization Mass Spectrometry
OPO : Optical Parametric Oscillator
SHG : Second Harmonic Generator
MCP : Micro Channel Plate
DSA : Digital Signal Averager

FIG. 15. Block diagram of RIMS system with TOF mass spectrometer.

The optical parametric oscillator (OPO) is excited using the YAG laser at the 355 nm wavelength. The higher harmonic wave is then generated from 512 nm OPO light in the secondary higher harmonic generator (SHG), and the laser-ionized sample gas flows into the ionization chamber. The ion is then detected in the micro channel plate (MCP), and it is counted by the digital signal averager (DSA). An example of measured data for sample argon gas containing 10 ppb of xenon with a natural isotopic distribution is shown in Fig. 16. A sharp mass spectrum was obtained by RIMS, which demonstrates a high sensitivity to the diluted cover gas in the order of few ppb.

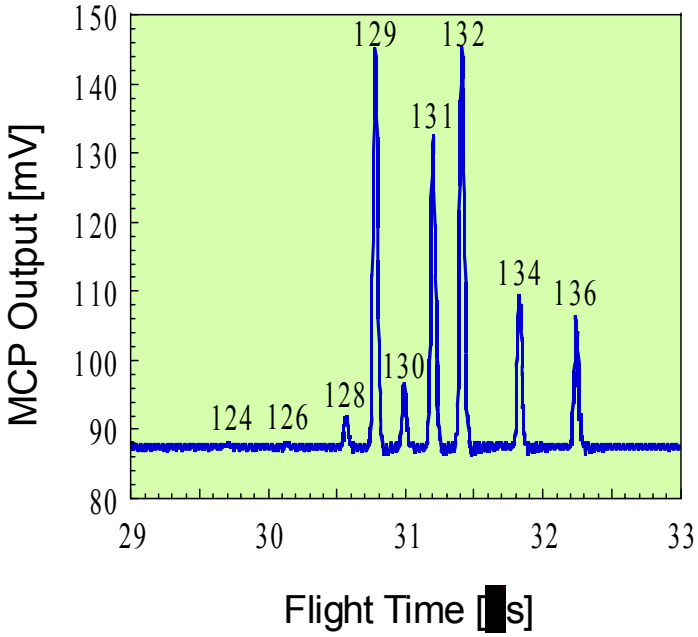

FIG. 16. Measured mass spectrum of natural xenon.

6.2. Installation of FP traps

Two types of FP traps have been installed in JOYO. One is a cesium trap installed in the primary coolant sodium purification system to capture cesium released from failed fuels. An open pore, foam-like glassy carbon that consists of thin struts of Reticulated Vitreous Carbon (RVC) is used as a material for collecting cesium. The capacity of this trap is designed to be 7.4E+12 Bq. The other trap is a Cover Gas Clean-up System (CGCS) to collect and store the noble fission gas released from failed fuels. Although it is planned that only one failed fuel pin will be in the core at any time, the CGCS is designed to handle the releases of up to twelve failed fuel pins.

6.3. Fuel failure simulation tests

An in-pile simulation test was carried out at the end of the 7th operational cycle using two artificially defected (slit) fuel pins to verify the performance of JOYO's FFDL system. This system uses the sodium sipping method. The slit is 1.0 mm long and 0.1 mm wide and perforated on the fuel cladding at gas plenum position. In the FFDL operation, a signal level of the test subassembly was several hundreds times higher than the background measured for other core subassemblies (Fig. 17). With this test, the FFDL system was confirmed to have the capability to identify the failed fuel with a defect at a gas plenum position. A FP source using U-Ni alloy tubes was irradiated at the end of 15th operational cycle. The test results show two important results. Both the CG and DN monitoring system were successfully calibrated and the CG monitor was confirmed to have enough sensitivity to the FP gas released from the failed fuel pins. The major constants for the cover gas and DN behavior models were determined and the disengagement rate constant of the FP gas from the sodium coolant to cover gas region varied depending on the flow rate of the primary cooling system.

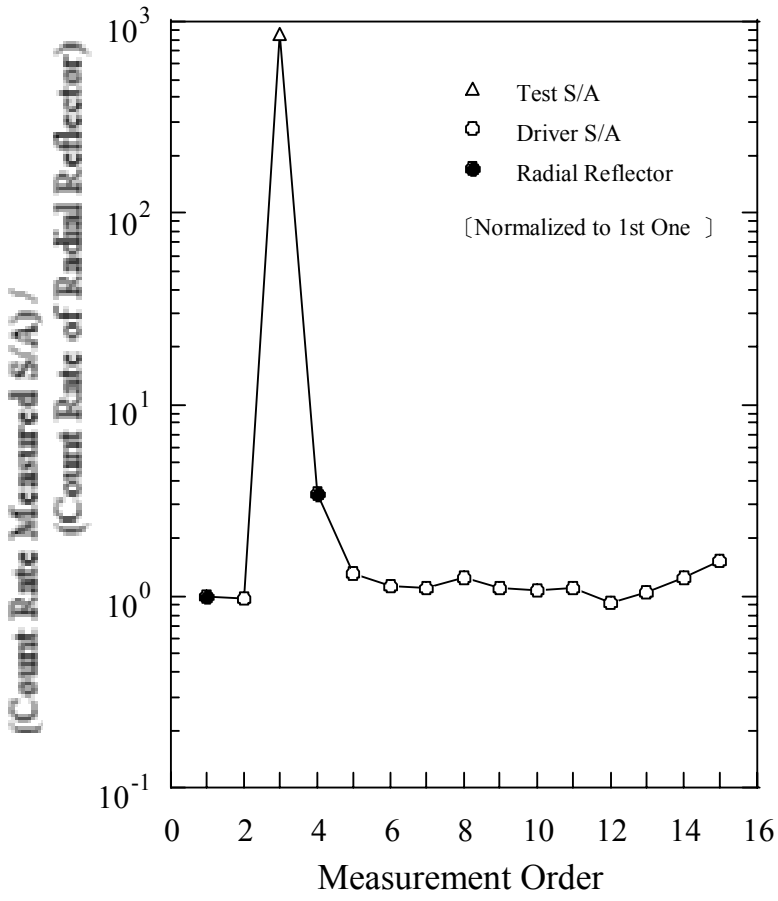

FIG. 17. Relative count rate of Xe-133 gamma-ray from examined subassembly.

7. MEASUREMENT OF RADIOACTIVE CORROSION PRODUCTS (CP)

The sodium cooled fast reactor JOYO has been operated more than 20 years (about 5 years of effective full power years) since its initial criticality and the cumulative reactor output achieved over 1.9E+5 MWd. Since JOYO has not yet experienced any operation with breached fuels, FP radioactive contamination has not become an issue in the plant system. To reduce the radiation dose from long-lived ^{22}Na, all primary coolant sodium in the main circulating loops is drained into a storage tank during annual plant inspections. Under these conditions, the spatial gamma-ray dose rate distribution is dominated by the radioactive CPs deposited on inner surfaces of the primary piping and components. This means that most personnel dose was due to these CPs.

7.1. Measured results and analysis

The CP deposits on the inner surfaces of the primary main piping have been measured at every annual inspection period since the end of MK-I operation in July 1982. These measurements are made at 14 locations, shown in Fig. 18, using a Ge solid-state detector system. The detector system was calibrated with a piping mock-up using two planer type standard gamma-ray sources, ^{54}Mn and ^{60}Co, so that the absolute amounts of CP deposits could be obtained from the measured gamma-ray spectra.

In every annual inspection, gamma-ray dose rates from these CP deposits have been measured using calcium sulfate (CaSO4) thermo-luminescence dosimeters (TLDs). The gamma-ray dose rate distribution near the piping is measured in detail at 93 locations at one-meter intervals along loop (A) from the outlet to the inlet of the reactor vessel. At each location, four TLDs are placed every 90 degrees around the thermal insulator cover. The geometrical conditions for the measurements are almost the same as those for the radioactive CP deposit mentioned above.

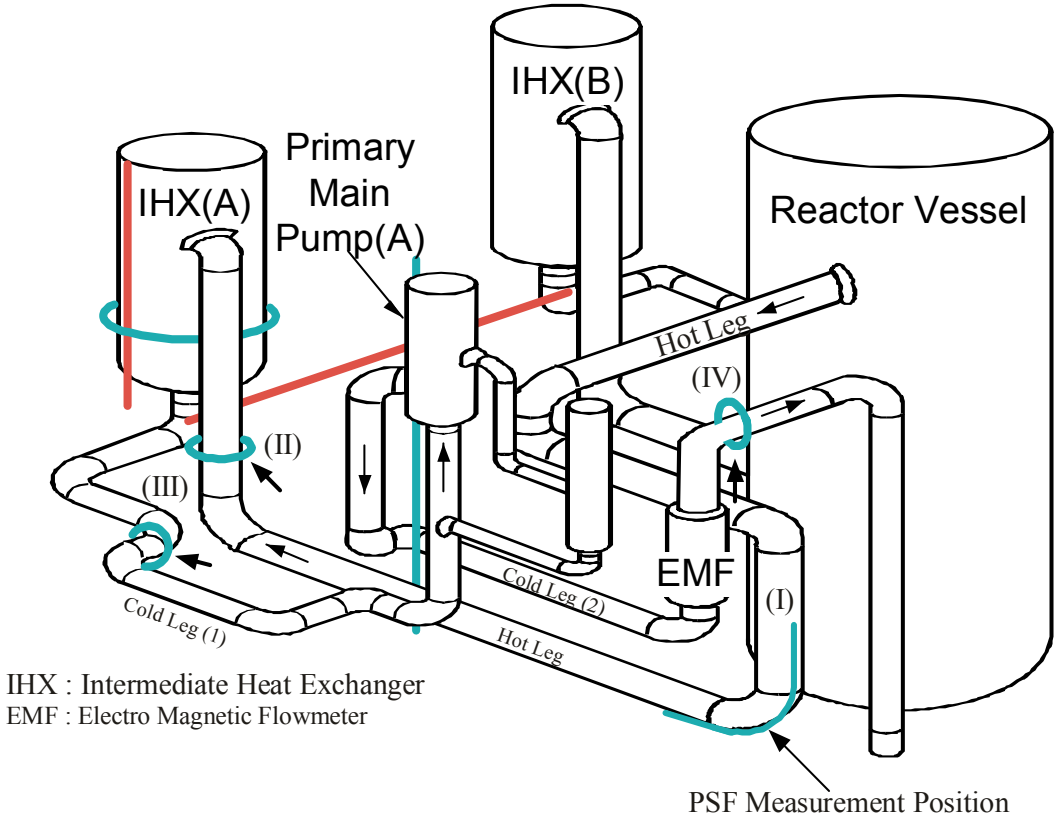

FIG. 18. Primary cooling loop of JOYO.

The CP behavior analysis code PSYCHE [13] has been developed and verified with the measured radiation data to analyze the distribution of corrosion product in the primary cooling system. A radiation dose calculation code has been developed by JNC, to analyze the CP deposition distribution along the piping and components of the primary cooling system. The build-up of CPs is shown in Fig. 19 together with the reactor operation time. The PSYCHE calculations agree with the measured values.

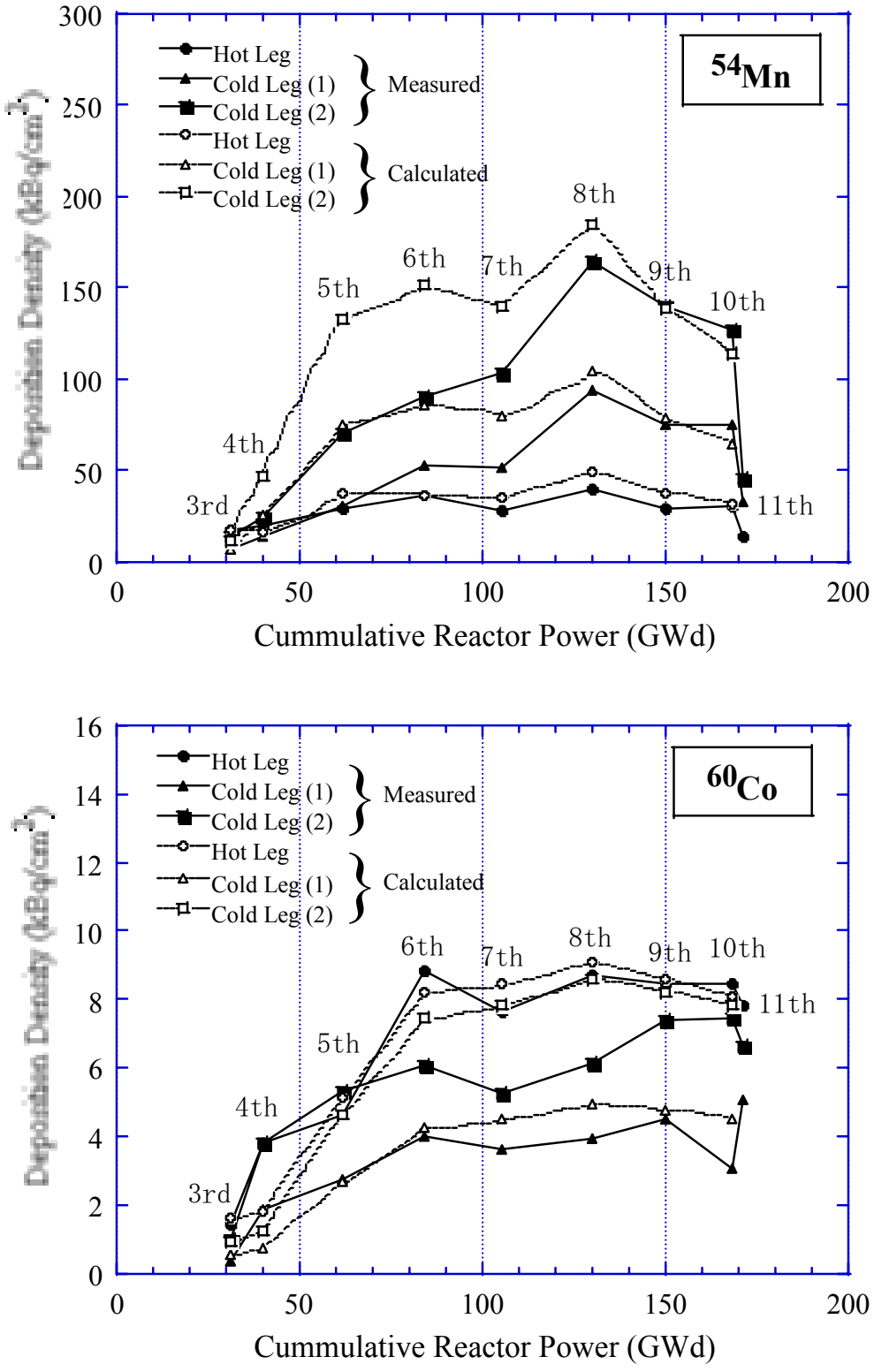

FIG. 19. Comparison of measured and calculated CP build-up in primary cooling piping (A).

7.2. Application of optical fiber

A Plastic Scintillation Fiber (PSF) measured the dose rate distribution in the primary cooling system of JOYO [14]. Figure 20 shows the schematic diagram of the PSF system.

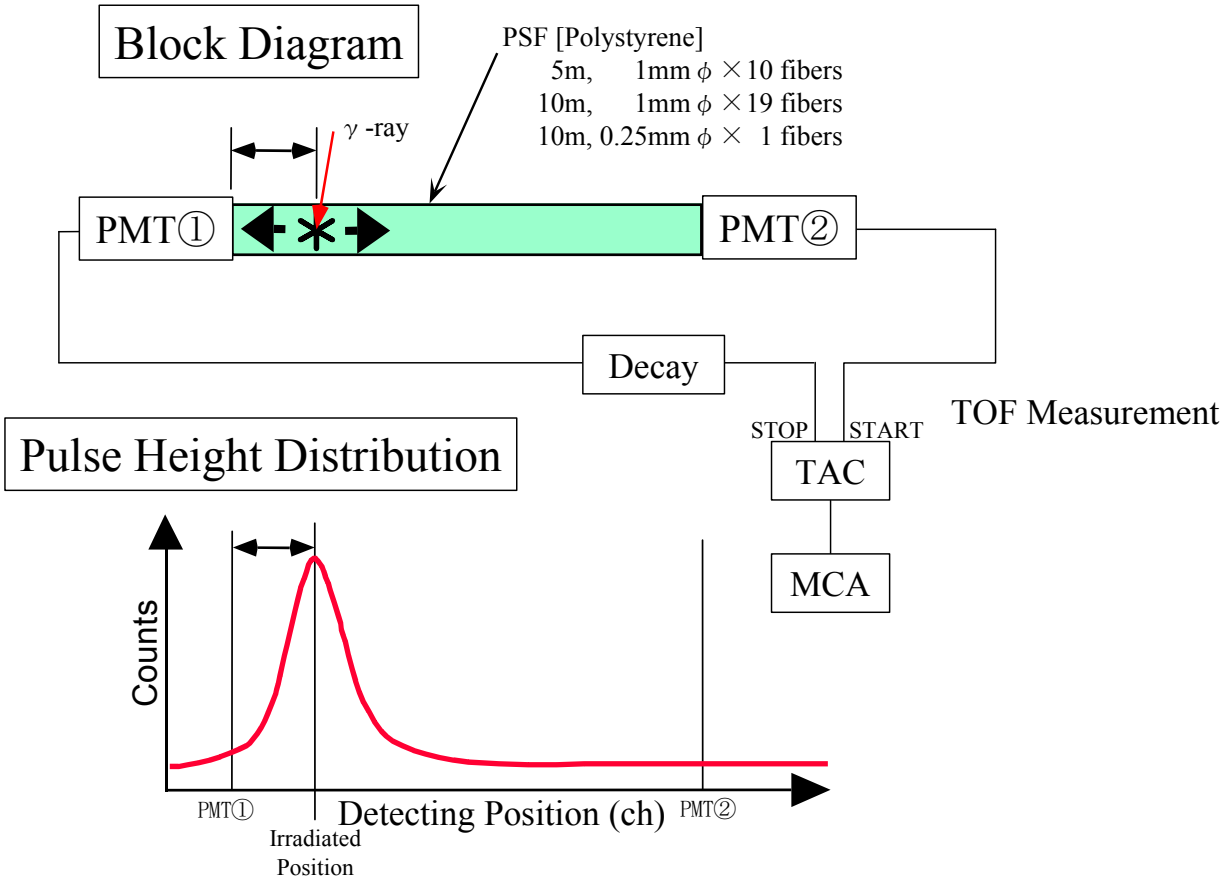

FIG. 20. Block diagram of radiation measurement using PSF.

Polystyrene was used as a scintillator that emits light in response to gamma-rays. The radiation source's location was determined with the time of flight method by measuring the time interval between the signals from two photo multipliers at each end of PSF. As seen from the pulse height distribution in Fig. 19, the measured count rate distribution does not have a sharp gradient even for a single point irradiation; therefore, the unfolding method is applied to reproduce the actual dose rate distribution.

The gamma-ray dose rate profile of the A loop IHX, shown in Fig. 21, is an example of the measured PSF data. Two peaks were observed due to horizontal plates in these positions where there were large CP deposits. Comparing PSF results with a series of TLD point data, large differences were observed at these peaks. However, by employing the unfolding method, the PSF data coincided with the TLD results. The gamma-ray dose rate distribution measurement was greatly improved by the use of PSF.

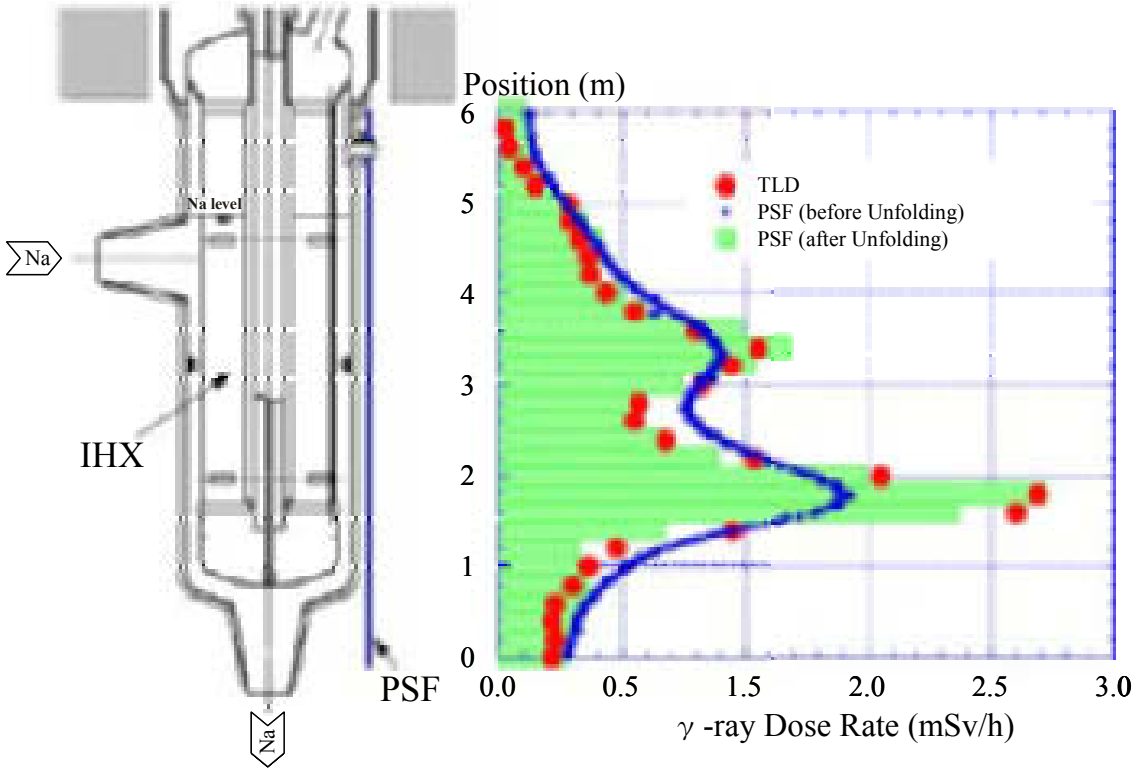

FIG. 21. Measured axial gamma-ray dose rate distribution of IHX.

8. OPERATION AND MAINTENANCE SUPPORT SYSTEMS

The JOYO operation and maintenance support systems ensure more stable operations and improve operational reliability. Artificial intelligence techniques [15] have been applied to develop these systems. One system objective is to support intelligent decision making by the operators and maintenance engineers, and another is to conduct skill-based and rule-based operator actions automatically. With proper instructions and guidance from the support system, the JOYO operators can make better decisions and carry out necessary actions with more confidence and less mental pressure.

8.1. Operation support system

The operation support system named JOYCAT (JOYO Conducting and Analyzing Tool) [16] was developed to help operators make intelligent and quick decisions in cases of anomalous event occurrences. Figure 22 illustrates the JOYCAT hardware configuration. The JOYCAT system consists of a knowledgebase and an inference system connected to the JOYO data acquisition system (JOYDAS). The JOYDAS collects on-line plant operation data from several thousands sensors located in different positions in the plant at interval of 0.25 second. Prior to its application to the JOYO plant, JOYCAT was validated by a full scope operator-training simulator. The alarm signals used for this validation were triggered by a manual scram during the reactor shut down process and by activating the reactor safety system during a periodic test. The system has been used since 1988.

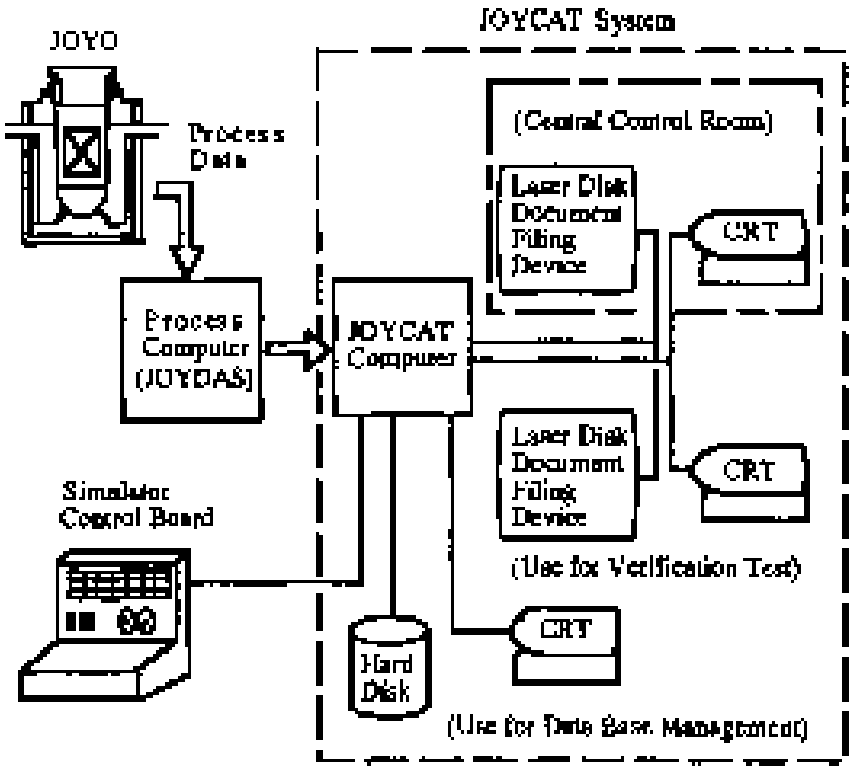

FIG. 22. JOYCAT hardware components.

The features of the JOYCAT system are:

- When an alarm occurs, the system diagnoses the plant conditions based on data from the reactor systems and the main components.
- Based on the system knowledge base, the alarm sequences and plant interlocks are checked. If nothing wrong is found, the system identifies the cause of the alarm. When an anomaly is found in some sequence or a safety system failure, the related information is displayed quickly on a CRT for the operators.
- After the cause of the alarm is identified, the most suitable operation manual for the anomaly is displayed for the operators.

8.2. Automatic control rod operation system

The JOYO operators control the reactor power, i.e. neutron flux level, by adjusting the position of the control rod subassemblies in the core. This is a manual operation performed from the central control room. To improve operational reliability as well as to reduce the mental load on the operators, an automatic control rod operation system [16] has been developed. This system has the following capabilities:

1) Drive the control rods;
2) Indicate the rod drive stroke for each control;
3) Indicate the criticality point (5E+4 cps for Source Range Monitor);

1) Drive the control rods;
2) Indicate the rod drive stroke for each control;
3) Indicate the criticality point (5E+4 cps for Source Range Monitor);
4) Monitoring of the reactor period, neutron flux, thermal output of the reactor, rate of reactor power change, heat-up rate at the reactor vessel inlet, and the temperature difference between the overflow tank and the reactor vessel outlet;
5) Guide the plant operation;
6) Display information concerning the rod operation and the current plant conditions, i.e. trend graphs of the thermal power, neutron flux and reactivity of the core.

In actual operation, the operator's actions in accordance with the above guidance should be conducted in a different manner depending on the reactor power level as described in Figure 23. A fuzzy algorithm based on linguistic rules is employed to control non-linear characteristics, whereas this is a difficult problem for the conventional PI controller.

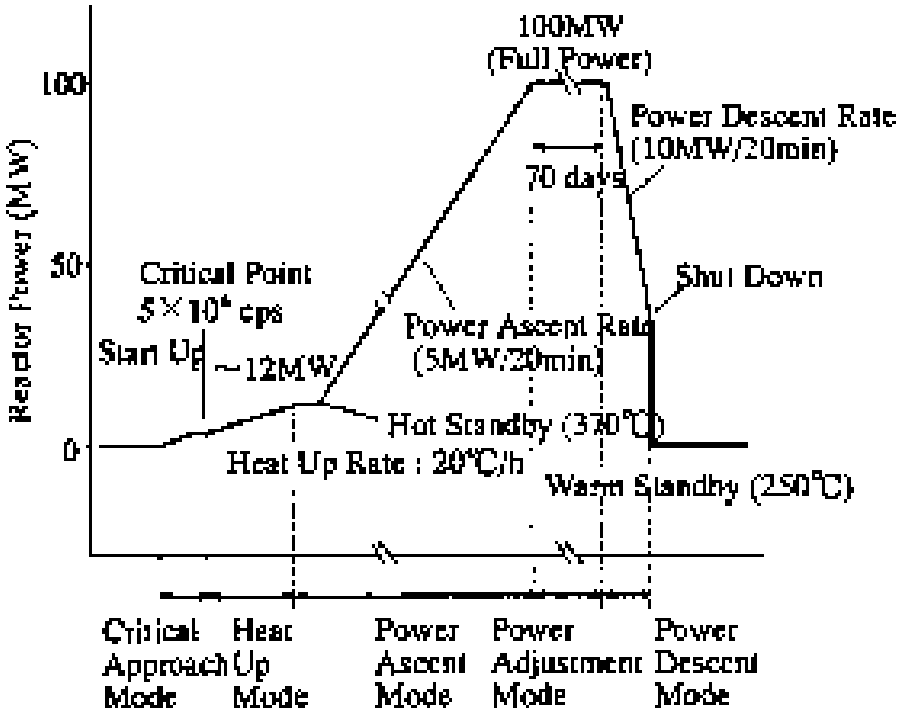

FIG. 23. Control mode of automatic control rod operation system.

In the past, the control rod drive stroke was calculated by the operators prior to manual control when approaching criticality. After the installation of the system, it calculates and displays an inverse multiplication curve and the stroke of each control rod subassembly that needs to be driven using the neutron flux and the vertical control rod position. The reliability of this system was validated during a complete operational cycle of the MK-II core. It was also demonstrated that the operation guides provided by the system were very similar to those chosen by the experienced JOYO operators.

8.3. Maintenance support system

High security and reliability of equipment is required in nuclear reactor plants. The equipment is designed based on failure analysis and preventive maintenance and condition monitoring are recommended. The condition monitoring technique has been developed to detect the failure and degradation of the machine as soon as possible to diagnose anomaly causes and to evaluate the machine's damage. The equipment is used under various stresses depending on their operating environments and these stresses cause degradation or failures such as fatigue, wear and tear, corrosion and others. In most cases, these appear as changes in vibration or acoustic noise so vibration monitoring is a popular and effective technique especially for rotating machines like motors or pumps.

In JOYO, a vibration monitoring systems named MEDUSA (MEchanical-fault Diagnosis Using Spectrum Analysis) [17] has been developed as an on-line vibration monitoring system for the major rotating machines such as the main pumps of the primary and secondary cooling systems. MEDUSA monitors the vibration of major rotating machines automatically and continuously, and it notifies plant operators and maintenance engineers of any anomalies it detects. Furthermore, the MEDUSA could assist in the analysis and interpretation of the vibration data.

8.3.1. System configuration

Figure 24 illustrates the system configuration of MEDUSA.

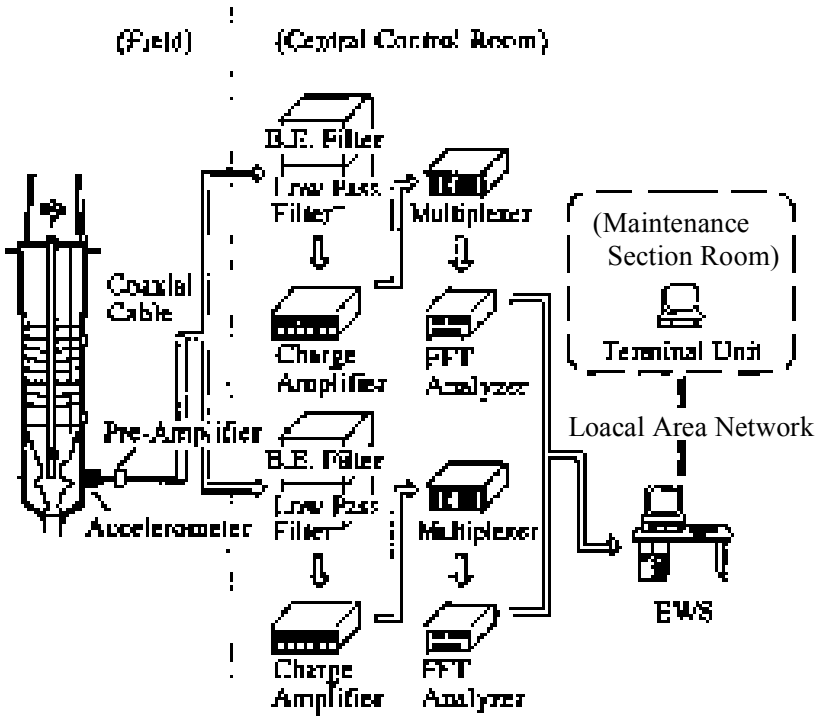

FIG. 24. System configuration of MEDUSA.

Vibration signals are collected by accelerometers mounted on each rotating machine and the signals are sent to the multiplexers (Fast Fourier Transform (FFT) analyzers) through the amplifiers and filters. The engineering work station (EWS) manages the instruments and vibration data. The FFT analyzers and multiplexers save the CPU load of the EWS for the signal processing so MEDUSA could easily deal with the increasing number of monitoring machines.

The MEDUSA monitors vibration levels (r.m.s. and peak levels), auto power spectrum densities (APSDs), waveforms and probability density functions at every hour automatically, then the r.m.s. levels and the APSDs are compared with acceptable vibration levels to judge whether the machine's condition is normal.

If an anomaly condition is detected, warning messages and beeps notify the plant operators and maintenance engineers. Monitoring intervals are variable and it is possible to monitor more frequently when an anomaly symptom is detected or for test runs after an inspection.

Vibration data has been kept for 300 days on the EWS, and the previous data is dumped into digital audiotapes. These data could be accessed on the terminals anytime, so that the follow-up survey over a long term is possible. Operators can review how an anomaly symptom appears and how it increases by a trend graph and a three dimensional graph (time-frequency-amplitude of vibration).

The characteristic vibration data for an anomaly condition of the rotating machine is saved with a label and description that includes phenomena, causes and measures against the anomaly. These data could be used as a reference to judge the machine condition and to make a necessary action.

8.3.2. Experience of vibration monitoring in JOYO

The MEDUSA has been used as a regular part of plant maintenance and operation since 1990, and it is useful to detect anomalies and to diagnose their causes. As an example of vibration monitoring in JOYO, the vibration level of a cooling blower suddenly increased by a factor of ten on 31st December 1992. This blower is placed in a nitrogen gas atmosphere and cannot be repaired while the reactor is operating.

Figure 25 shows the APSD of vibrations before and after the increase of vibration. The vibration increased in higher frequency region over 5 kHz (increased -50 dB to -20 dB around 6 kHz). Therefore, it was estimated that the vibration occurred due to loss of lubrication oil or bearing failure.

Later at the annual inspection of the blower, it was found that there was a loss of lubrication oil in the bearing box and the vibration level decreased after refilling the oil.

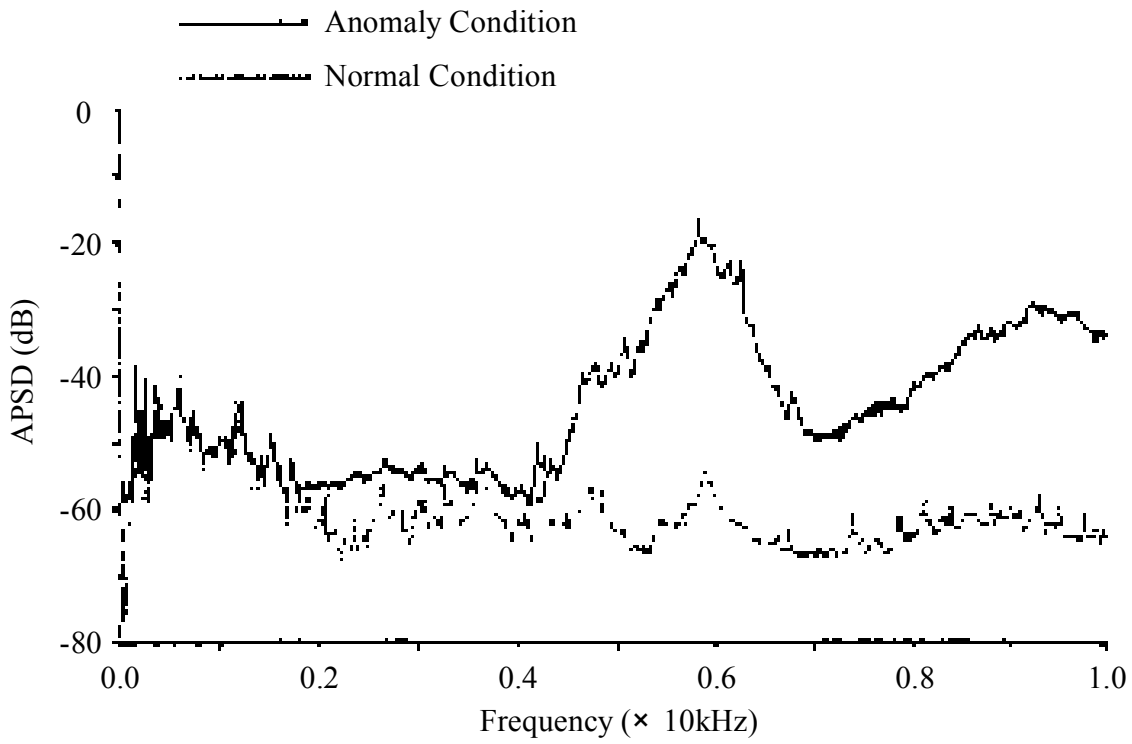

FIG. 25. Comparison of vibration spectra (loss of lubricating oil).

9. IMPROVEMENT OF COUNTERMEASURES AGAINST SODIUM LEAKS

A sodium leak accident occurred in the MONJU secondary cooling loop in December 1995. At that time, the 11th annual inspection was being performed at JOYO and an inspection of sodium piping and components was immediately carried out to confirm their integrity and to verify that there were no sodium leaks. After the MONJU accident, an investigation was completed by the Safety Authority and findings on the cause of the sodium leaks and ways to mitigate their effects were published.

According to this report, the structural integrity of the JOYO thermocouple well was tested and confirmed by hydraulic vibration evaluation based on water flow tests and ASME standards. Modifications were then made at JOYO to improve countermeasures against sodium leaks in the secondary loop [18].

The improvements of these sodium leak countermeasures in the secondary loop stressed prevention, early detection and mitigation of the effects. The improvements were determined according to the following considerations:

(1) Sodium leak prevention

- All the thermocouples in the secondary loop were inspected by non-destructive examination (X-ray, fiber scope inspection) to confirm their integrity.
- All the thermocouples were replaced by new ones with compression fittings that seal any sodium leaking between the thermocouple well and sheath in the event of a thermocouple well rupture.

(2) Early detection of sodium leaks

- A new sodium leak monitor was installed in the central control room to verify the function of each sodium leak detector.
- A new fire alarm monitor was installed in the central control room to verify the function of each fire detector. This monitor has a second alarm function that re-alarms if another detector goes off.
- Monitor cameras were installed in the secondary cooling facility to view the sodium piping and components from the central control room.

(3) Mitigation of sodium leak effect

- Sodium leak trays were added under the sodium piping to prevent dispersion of leaking sodium.
- Anti-smoke dampers were added in the ventilation system to prevent the diffusion of sodium aerosol. The dampers in the ventilation system are interlocked with the sodium leak detector and fire detector to shut automatically.
- The penetration gaps between the piping and walls were sealed to prevent the diffusion of sodium aerosol.

(4) Improvement of Manuals

- Upgrade of Operational Manuals.
  i. The emergency operational manual for JOYO sodium leaks was reviewed and verified as valid.
  ii. The emergency operational manual was upgraded by incorporating the improved countermeasures against sodium leaks.
- Revision of education and training schedule
  ii. Emergency operation training, sodium fire-extinguishing training and overall disaster prevention training have been carried out.
  iii. The education and training schedule was revised to provide more skilled training.

JOYO's safety practice for sodium leaks were investigated by the Safety Authority. After a successful investigation, JOYO was allowed to restart operations in March 1997.

10. UPGRADING PROGRAM AND MODIFICATION OF CORE AND COOLING SYSTEM COMPONENTS

JOYO is expected to play a greater role in providing an irradiation field for fuels and materials irradiation tests and for the demonstration of innovative safety related systems for future fast reactors. To meet the increasing requirements for the various irradiation tests, the JOYO MK-III upgrading program was initiated to improve its irradiation capability [18 – 20]. The main objectives of the MK-III program are to increase the neutron flux, modify the

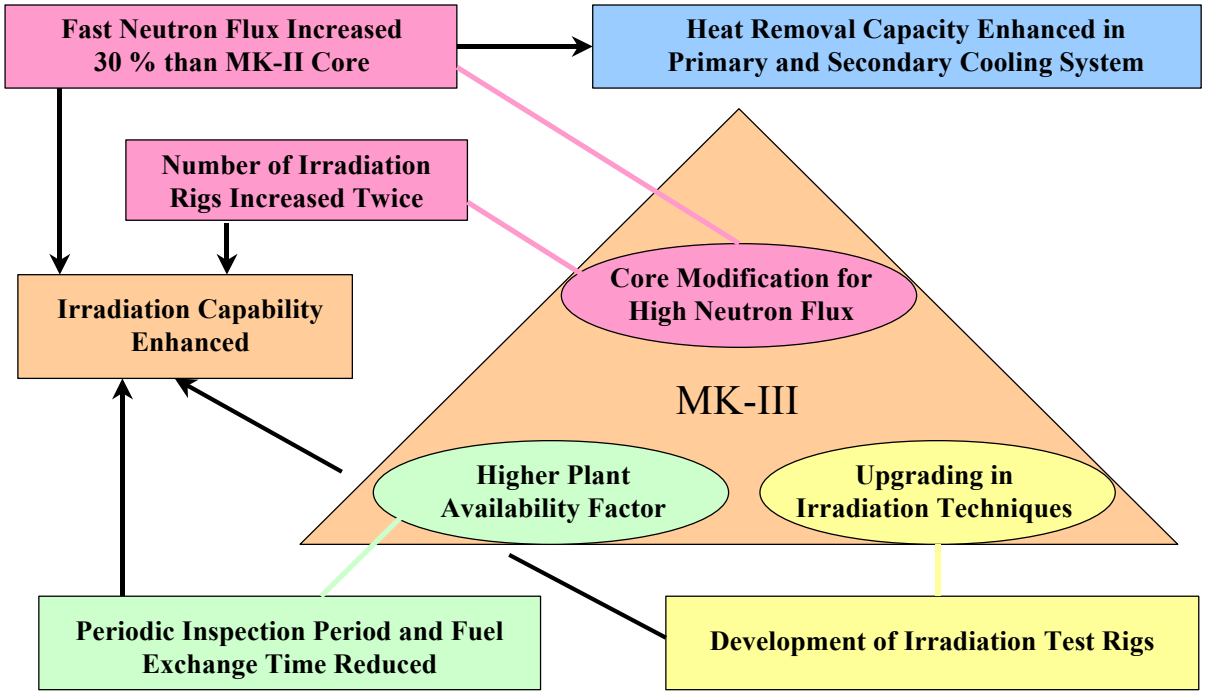

FIG. 26. Main purpose of MK-III project.

10.1. Outline of MK-III project and specification

The basic specifications of JOYO are previously shown in Table 1, which compares the MK-II and MK-III cores. The MK-III core is divided into two regions with different plutonium contents and the core height is decreased from 55 to 50 cm to obtain higher neutron flux with smaller power peaking. Two of six control rods are shifted to the edge of the outer core to enlarge the high neutron flux irradiation field. Two layers of radial stainless steel reflector are replaced by the shielding subassemblies, which contain boron carbide pellets, to reduce the neutron dose in the radial direction.

A whole plant design optimization increases the reactor thermal output from 100 to 140 MWt. The fast neutron flux increases about 30% as shown in Fig. 27 and the maximum allowable number of fuel irradiation test rigs increases from nine to twenty-one. The MK-III core will support various irradiation tests on advanced fuels like MA doped fuel, high plutonium content MOX fuel and vibration packed fuel. The irradiation technology has also been developed to expand the capability and flexibility of fuels and materials irradiated.

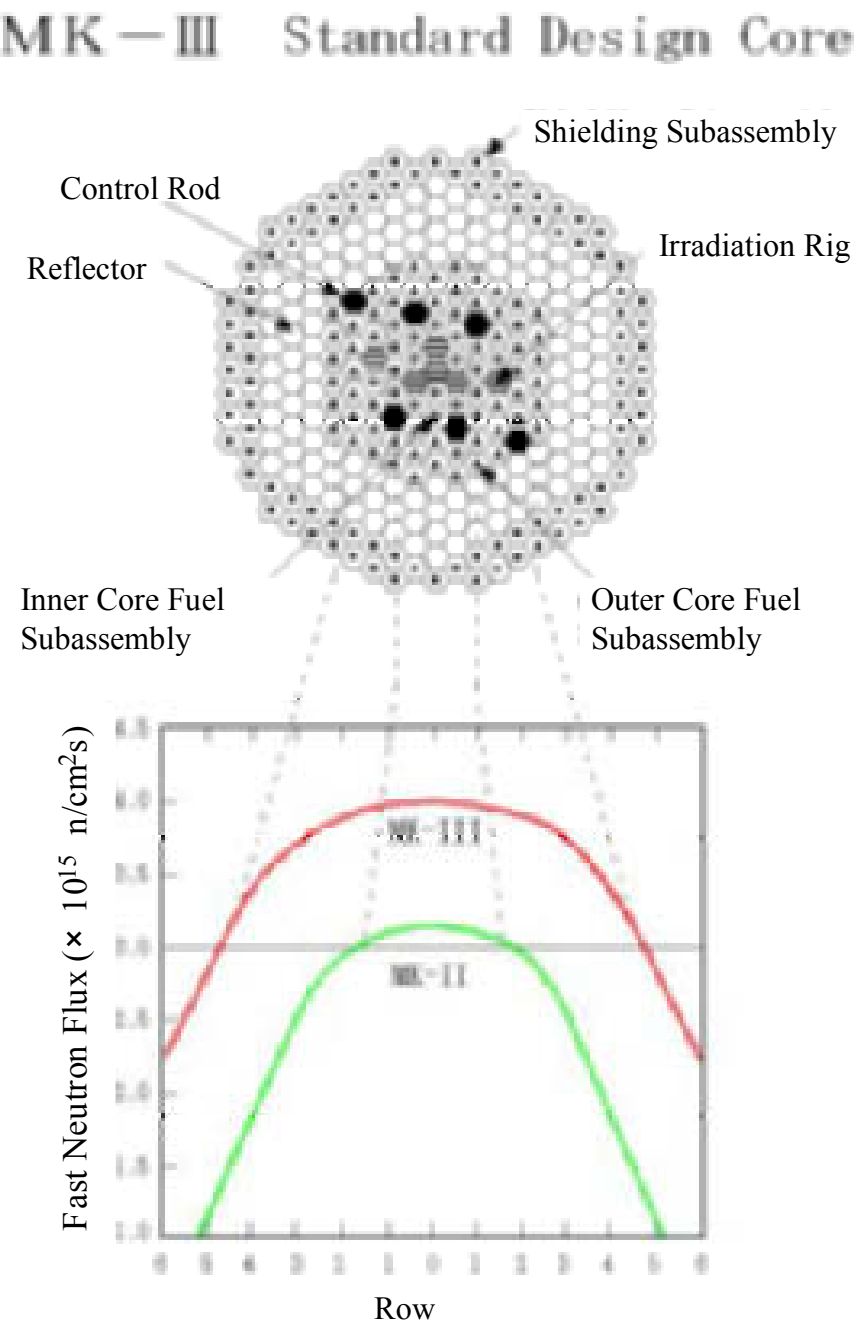

FIG. 27. Core configuration and fast neutron flux distribution in MK-III core.

The JOYO cooling systems need to be modified to increase the heat removal capacity. Figure 28 shows the components to be exchanged in the modifications and compares the plant condition in the cooling system. The primary system sodium coolant flow rate increases by 20% and all Intermediate Heat Exchangers (IHX) and Dump Heat Exchangers (DHX) were replaced. The cooling system modification completed in September 2001 and the cooling systems were refilled with sodium then the initial purification was conducted. The cold trap in the secondary sodium purification system will be replaced in the autumn of 2002.

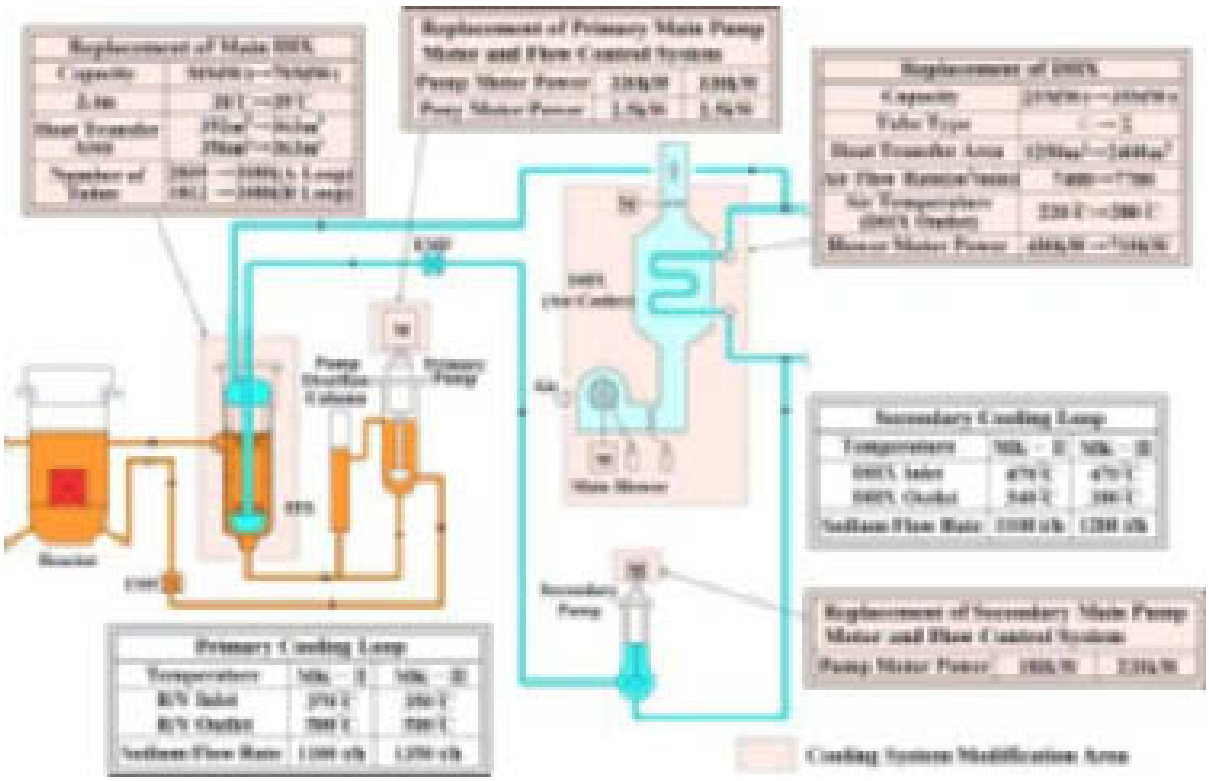

FIG. 28. Cooling system components to be exchanged.

10.2. Modification work experience

Special attention was given to prevent air containment when cutting the sodium boundary during this modification work. The following procedure was employed for replacing the DHX. First, the temporary supports for sodium piping and argon gas supply lines were installed in preparation for cutting the sodium piping. Next, the sodium piping was cut to two-thirds of their thickness using the cutting tools. A glove box was installed to cover the sodium piping cuts to keep the cover gas boundary filled with argon.

The sodium piping was cut off after a leak test was conducted. The sodium on the inner surface of the cutting part was scraped off and the residues were rinsed with alcohol. After the shut-off plug was set in the inner part of the piping to completely shield it, the beveling of the welding part was done to prepare for the new piping weld. Since all the cutting positions of the sodium piping are horizontal, the cutting powder from the piping is relatively easy to collect, preventing it from entering in the cooling system. In this way, all the sodium piping was cut off using the cutting bits.

The cover gas pressure in the secondary argon gas system at normal operation is controlled in the range of 34 to 44 kPa. It was decided to lower the cover gas pressure to 220 Pa at for the cutting work based on the experience of taking the surveillance materials out of the system, and the glove box pressure ratings. An automatic low-pressure argon control system was newly installed in the system. The oxygen concentration inside the glove box was controlled below the level of 1000 ppm. The control value of oxygen and nitrogen concentration in the system sodium piping is below 300 and 1200 ppm, respectively.

10.3. Future schedule

The performance of newly installed components and cooling systems will be confirmed through a series of functional system tests. The core replacement will start in the summer of 2002. When the initial MK-III core configuration is complete, the reactor power will be increased in steps to conduct performance tests that confirm the core physics and plant characteristics. The MK-III rated power operation will start in 2003.

11. CONCLUSIONS

The successful operations of JOYO provide a wealth of experiences with core management, impurity control, reactor engineering tests, innovative instrumentation techniques, operation and maintenance support systems, and component modifications. These experiences and accumulated data are to be used for the design of future fast reactors. They are also useful for upgrading the JOYO core and plant to the MK-III configuration and are essential to secure steady and safe reactor operation and enhance the irradiation capability of JOYO in the future.

REFERENCES

[1] MAEDA, S., et al., Fast Reactor Core Management in Japan: Twenty Years Evolution at JOYO, Proc. 5th International Topical Meeting on Research Reactor Fuel Management (RRFM 2001) Eurogress Aachen, Germany, 1-4 April 2001, European Nuclear Society (ENS) (2001) pp. 56-60.

[2] TABUCHI, S., AOYAMA, T., Development of JOYO MK-II Core Characteristics Database, Proc. Symp. on Nuclear Data, Ibaraki, Japan, 18-19 November 1999, Naoki Yamano and Tokio Fukahori (Eds), JAERI-Conf 2001-006 (2000) pp. 149-153.

[3] TAKANO, H., KANEKO, K., Revision of Fast Reactor Group Constant Set JFS-3-J2, JAERI-M 89-141 (1989).

[4] NAKAGAWA, T., et al., Japanese Evaluated Nuclear Data Library Version 3 Revision-2: JENDL-3.2, J. Nucl. Sci. Technol., **32**, 12 (1995) p. 1259.

[5] TAKAMATSU, M., AOYAMA, T., Neutron Intensity of Fast Reactor Spent Fuel, Proc. Symp. on Nuclear Data, Ibaraki, Japan, 27-28 November 1997, Tadasi Yoshida and Tokio Fukahori (Eds), JAERI-Conf 99-002 (1998) pp. 21-26.

[6] Atom Percent Fission in Uranium and Plutonium Fuel (Neodymium) Annual Books of ASTM Standard, E-321-79 (1971).

[7] MAEDA, S., AOYAMA, T., Decay Heat of Fast Reactor Spent Fuel, Proc. Int. Conf. on Nuclear Data (ND2001), Ibaraki, Japan, 7-12 October 2001, JAERI, published as Journal of Nuclear Science and Technology, Supplement 2 (2002).

[8] TASAKA, K., et al., JNDC Nuclear Data Library of Fission Products -Second Version-, JAERI 1320 (1990).

[9] SAWADA, M., et al., Experiment and Analysis on Natural Convection Characteristics in the Experimental Fast Reactor JOYO, Nuclear Engineering and Design, **120** (1990) pp. 341-347.

[10] AOYAMA, T., et al., The Operational Experience of the Experimental Fast Reactor JOYO, Proc. 3rd Asian Symposium on Research Reactor, Ibaraki, Japan, 11-14 November 1991, JAERI (1991) pp. 75-82.

[11] AOYAMA, T., ITO, C., Integral Test on Activation Cross Section of Tag Gas Nuclides Using Fast Neutron Spectrum Fields, Proc. Int. Conf. on Nuclear Data (ND2001), Ibaraki, Japan, 7-12 October 2001, JAERI, published as Journal of Nuclear Science and Technology, Supplement 2 (2002).

[12] WATANABE, K., et al., Development of Failed Fuel Detection and Location Technique Using Resonance Ionization Mass Spectrometry, J. Nucl. Sci. Technol., **38**, 10 (2001) pp. 844-849.

[13] IIZAWA, K., et al., Transport of Radioactive Corrosion Product in Primary Systems of a Sodium Cooled Fast Reactor, Proc. Material Behavior and Physical Chemistry in Liquid Metal Systems 2, Plenum Press, ISBN 0-306-45069-0 (1995) pp. 9-26.

[14] AOYAMA, T., et al., Application of Optical Fiber for Radiation Measurement in Fast Reactor Primary Cooling System, Proc. 12th Pacific Basin Nuclear Conference, Seoul, Korea, 29 October – 2 November 2000, Vol. 2, Korea Atomic Industrial Forum and Korea Nuclear Society (KAIF-KNS) (2000) pp. 095-1105.

[15] HIMENO, Y., et al., Improvement of Man-Machine Interaction by Artificial Intelligence for Advanced Reactors, Reliability Engineering and System Safety, **38** (1992) pp. 135-144.

[16] SAWADA, M., et al., Operation and Maintenance Support Systems of the Experimental Fast Reactor JOYO, Proc. Int. Topical Meeting on Safety of Operating Reactors, Seattle, USA, 17-20 September 1995, ANS (1995) 564-570.

[17] UEDA, M., et al., Condition Monitoring System of Rotating Machines in the Experimental Fast Reactor JOYO, Proc. 3rd JSME/ASME Joint Int. Conf. on Nuclear Engineering (ICONE-3) Kyoto, Japan, 23-27 April 1995, Vol. 3, ASME (1995) pp. 1619-1621.

[18] MAEDA, Y., et al., Current Status and Upgrading Program of the Experimental Fast Reactor JOYO, Proc. World Nuclear Congress and Expo (ENC'98) Trans., Nice, France, 25-28 October 1998, Vol. IV, Workshops, (1998) pp. 21-30.

[19] SUZUKI, S., et al., Upgrading Program of the Experimental Fast Reactor 'JOYO' - The MK-III Program -, Proc. 10th Pacific Basin Nuclear Conference, Kobe, Japan, 20-25 October 1996, Vol. 1, Atomic Energy Society of Japan (AESJ) (1996) pp. 759–768.

[20] YOSHIDA, A., et al., Upgrading Program of the Experimental Fast Reactor Joyo, Book of Abstracts Int. Conf. on Nuclear Engineering (ICONE-9), Nice, France, 8-12 April 2001, Vol. 2, ASME (2001) p. 492.